# Semicentennial Response of a Bifurcation Region in an Engineered River to Peak Flows and Human Interventions

Chowdhury, M. Kifayath; Blom, Astrid; Ylla Arbós, Clàudia; Verbeek, Merel C.; Schropp, Max H.I. ; Schielen, Ralph M.J.

**DOI**
10.1029/2022WR032741

**Publication date**
2023

**Document Version**
Final published version

**Published in**
Water Resources Research

**Citation (APA)**
Chowdhury, M. K., Blom, A., Ylla Arbós, C., Verbeek, M. C., Schropp, M. H. I., & Schielen, R. M. J. (2023). Semicentennial Response of a Bifurcation Region in an Engineered River to Peak Flows and Human Interventions. *Water Resources Research*, *59*(4), Article e2022WR032741. https://doi.org/10.1029/2022WR032741

AGU ADVANCING EARTH AND SPACE SCIENCE

Water Resources Research

RESEARCH ARTICLE
10.1029/2022WR032741

# Semicentennial Response of a Bifurcation Region in an Engineered River to Peak Flows and Human Interventions

**M. Kifayath Chowdhury[1], Astrid Blom[1], Clàudia Ylla Arbós[1], Merel C. Verbeek[2], Max H. I. Schropp[2], and Ralph M. J. Schielen[1,2]**

[1]Faculty of Civil Engineering and Geosciences, Delft University of Technology, Delft, The Netherlands, [2]DG Rijkswaterstaat, Ministry of Infrastructure and Water Management, Utrecht, The Netherlands

**Key Points:**

- Water discharge in one branch at a Dutch Rhine bifurcation has slowly increased at the expense of the other bifurcate
- This slow change in flow partitioning is associated with one bifurcate eroding faster than the other bifurcate
- Sudden deposition in one bifurcate (due to rapid succession of peak flows and sediment flux coarsening) likely triggered these changes

**Supporting Information:**

Supporting Information may be found in the online version of this article.

**Correspondence to:**

M. K. Chowdhury,
m.k.chowdhury@tudelft.nl

**Citation:**

Chowdhury, M. K., Blom, A., Ylla Arbós, C., Verbeek, M. C., Schropp, M. H. I., & Schielen, R. M. J. (2023). Semicentennial response of a bifurcation region in an engineered river to peak flows and human interventions. *Water Resources Research*, *59*, e2022WR032741. https://doi.org/10.1029/2022WR032741

Received 6 MAY 2022
Accepted 4 APR 2023

**Author Contributions:**

**Conceptualization:** M. Kifayath Chowdhury, Astrid Blom, Ralph M. J. Schielen
**Data curation:** M. Kifayath Chowdhury
**Formal analysis:** M. Kifayath Chowdhury, Clàudia Ylla Arbós
**Funding acquisition:** Astrid Blom, Ralph M. J. Schielen
**Investigation:** M. Kifayath Chowdhury, Astrid Blom, Ralph M. J. Schielen
**Methodology:** M. Kifayath Chowdhury
**Project Administration:** Astrid Blom, Ralph M. J. Schielen



**Abstract** A bifurcation in an engineered river system (i.e., fixed planform and width) has fewer degrees of freedom in its response to interventions and natural changes than a natural bifurcation system. Our objective is to provide insight into how a bifurcation in an engineered river responds to peak flows and human interventions. To this end, we analyze the change in hydraulics, bed level, and bed surface grain size in the region of two bifurcations in the upper Rhine delta in the Netherlands over the last century. We show that, over the last two decades, the water discharge in one bifurcate (the Waal branch) has steadily increased at the expense of the other. This gradual increase in the water discharge of the first branch is associated with its erosion rate being larger than the other branch. The quick succession of two or three peak flow events (1993, 1995, and 1998) caused rapid sediment deposition over the upstream part of the bifurcate that has gradually lost discharge, which seems to have triggered the slow change in flow partitioning.

**Plain Language Summary** A river bifurcation is where a river splits into two branches. Water and sediment from the upstream channel are divided between the bifurcation's downstream branches. This division is important for flood risk, freshwater supply, and navigation. Here we investigate the flow division and related changes in bed level and bed surface grain size in the bifurcation region in the upper Rhine delta in the Netherlands over the last century. We find that, over the last two decades, one branch (the Waal branch) has gradually received a larger share of the water discharge at the expense of the other branch. This gradual increase in the water discharge of the first branch seems to be associated with its erosion rate being larger than the other branch. This slow change in the division appears to be triggered by two or three successive peak flows (1993, 1995, and 1998), which caused sediment to deposit at the upstream end of the branch that subsequently started losing discharge gradually. Our analysis shows that peak flows can play a large role in bifurcation development in engineered river systems.

## 1. Introduction

Primary controls of channel response in an alluvial river system are the flow duration curve, downstream base level, and grain size-specific sediment supply (Blom et al., 2016; Blom, Arkesteijn, et al., 2017; Gilbert, 1877; Lane, 1955; Mackin, 1948). A change of these controls modifies the equilibrium state, resulting in channel adjustment toward this new equilibrium state. The equilibrium channel characteristics comprise the channel bed slope, channel width, and bed surface grain size distribution or surface texture. Here we consider engineered river systems (i.e., rivers where planform and width are fixed). Such fixed planform and banks limit the degrees of freedom for a channel to respond to natural change or human interventions. As a result, an engineered river responds through adjustment of channel slope by tilting and changing bed surface texture.

Bifurcations exist where the water discharge and sediment flux of a single channel are partitioned over two branches or bifurcates. They occur in environments such as deltas, braided and anabranching rivers, lowland rivers, and alluvial fans (Kleinhans et al., 2013). The partitioning of water and sediment at a bifurcation affects the larger river system, as the river bifurcation is the upstream boundary regarding water discharge (Arkesteijn et al., 2019) and sediment flux (Bolla Pittaluga et al., 2003; Wang et al., 1995) for the bifurcates and the downstream boundary for the upstream reach. The latter is affected by the bifurcation through backwater effects (Arkesteijn et al., 2019). The sediment partitioning depends on, for instance, the upstream water discharge, branch width (Wang et al., 1995), transverse bed slope (Bolla Pittaluga et al., 2003), bifurcation angle (Dutta et al., 2017), branch slope and planform upstream (Kleinhans et al., 2008) (see Schielen and Blom (2018) for an extensive list).

**Resources:** Astrid Blom, Ralph M. J. Schielen
**Supervision:** Astrid Blom, Merel C. Verbeek, Max H. I. Schropp, Ralph M. J. Schielen
**Visualization:** M. Kifayath Chowdhury, Astrid Blom, Clàudia Ylla Arbós, Ralph M. J. Schielen
**Writing – original draft:** M. Kifayath Chowdhury
**Writing – review & editing:** M. Kifayath Chowdhury, Astrid Blom, Clàudia Ylla Arbós, Merel C. Verbeek, Max H. I. Schropp, Ralph M. J. Schielen

River channels respond to peak flows in several ways: (a) deepening of narrow reaches accompanied by deposition in wide sections (Cenderelli & Wohl, 2003; Hauer & Habersack, 2009; Sholtes et al., 2018); (b) channel bed erosion in backwater reaches associated with a more or less constant base level alternating with deposition under base flows (Arkesteijn et al., 2019; Chatanantavet & Lamb, 2014; Chatanantavet et al., 2012); (c) sediment deposition in floodplains resulting from overbank flow (McKee et al., 1967; Ten Brinke et al., 1998); (d) outer bank erosion and inner bank deposition (Parker et al., 2010; Pizzuto, 1994; Van de Lageweg et al., 2014); and (e) in some cases channel widening (Huckleberry, 1994; Yousefi et al., 2018).

In natural river systems, peak flows can cause significant changes in bifurcation planform and width (Bertoldi, 2012). The supply of bed material load from upstream increases, and sediment waves migrate into the bifurcation area (Frings & Kleinhans, 2008). Peak flows can initiate avulsions, creating a bifurcation or a new river course (Kleinhans et al., 2013; Syvitski & Brakenridge, 2013). Engineered bifurcation systems typically do not allow for such planform change, so that their response is limited to change in bed level and bed surface texture. Observations over the Pannerdense Kop bifurcation of the Rhine River during a peak flow event in 1998 illustrated dune migration, scour upstream of the bifurcation, and hysteresis of bedload and suspended load transport (Frings & Kleinhans, 2008; Kleinhans et al., 2007). Rapid succession of peak flows can influence sediment transport rates in gravel bed rivers (Mao, 2018), and dune sorting may influence bed surface and subsurface texture by forming remnant gravel layers at the base of dunes or re-entraining them (Blom et al., 2003; Kleinhans, 2005).

Wang et al. (1995) were the first to illustrate that a bifurcation system with two bifurcates is not necessarily stable. Here, stable indicates a configuration where both bifurcates remain open with no systematic change of flow and sediment partitioning over time, and unstable means a configuration where one branch is characterized by an increasing discharge at the expense of the other branch. Such instability is associated with sediment deposition in one bifurcate and, eventually, its abandonment (Kleinhans et al., 2013; Schielen & Blom, 2018). The associated timescale of closure varies largely (Kleinhans et al., 2013).

A prime example of an engineered river is the Rhine River. It flows from the Swiss Alps to the North Sea and is among the most heavily engineered river systems in the world. River training along the Rhine in the 19th and 20th centuries comprised channel narrowing by 30%–40% (Havinga, 2020; Hesselink, 2002; Van de Ven, 1976; Wolfert, 2001; Ylla Arbós et al., 2021), which has resulted in a decrease of the equilibrium channel slope (Ylla Arbós et al., 2021). This is because, in a narrower channel, a smaller slope suffices to transport the supplied sediment downstream (Blom et al., 2016; Blom, Arkesteijn, et al., 2017; De Vriend, 2015; Mackin, 1948). The decrease of the equilibrium slope results in channel bed erosion (De Vriend, 2015; Quick et al., 2020; Visser, 2000; Ylla Arbós et al., 2021). Similar channel incision has been observed in other engineered rivers such as the Mississippi (Alexander et al., 2012), Rhône (Petit et al., 1996), and Danube (Habersack et al., 2016). Furthermore, the channel bed surface has coarsened with time (Frings et al., 2009; Ylla Arbós et al., 2021).

The upper Rhine delta in the Netherlands has two bifurcations, the Pannerdense Kop or Pannerden bifurcation and the IJsselkop bifurcation. Our objective is to provide insight on the response of this engineered river bifurcation system to peak flows and human interventions. We choose this system as a case study because of its long history of interventions and availability of field data for over half a century. We address the following research questions: (a) How has the bifurcation region in the upper Rhine delta developed (regarding flow partitioning, bed level, and bed surface grain size) over the last century? and (b) Which role have peak flows had in this development? To answer these questions, we inventorize past interventions and analyze field observations on bed level, bed surface grain size, and hydraulics over the last century. Section 2 describes the field site, past interventions, and flow duration curve. Results are subdivided among flow and sediment partitioning over the bifurcates (Section 3), change in bed level (Section 4), change in bed surface grain size (Section 5), and sediment supply versus sediment transport capacity (Section 6).

## 2. Field Site

We use the name Lower Rhine to indicate the set of Rhine River reaches of the Niederrhein (Germany), Bovenrijn, Waal, Nederrijn-Lek, and IJssel branches (Figure 1). The Niederrhein is the downstream part of the German Rhine, which enters the Netherlands near Lobith (river km 858), from where it is called the Bovenrijn. The Dutch part of the Rhine basin is known as the Rhine delta.

The Bovenrijn bifurcates into the Waal and Pannerden Canal branches at the Pannerden bifurcation (river km 867.5), the latter of which is located 10 km downstream of the German-Dutch border. We refer to the 11 km reach

**Pannerden Canal-Nederrijn-Lek**

| Year | River km | Intervention |
|---|---|---|
| 1707 | 868-878 | Opening of Pannerden Canal (PC) |
| 1773-1782 | 867,878 | Modification of IJsselkop and Pannerdense Kop |
| 1870-1890 | 867-970 | Narrowing: PC to 170 m and Nederrijn-Lek to 150 m |
| 1929-1934 | 867-970 | Narrowing: PC to 140 m and Nederrijn-Lek to 130 m |
| 1900-2002 | 867-947 | Dredging of sand and gravel. |
| 1953 | 867-878 | Modification of the PC (230 m shorter) |
| 1954-1958 | 947 | Construction of Hagestein weir |
| 1959-1966 | 922 | Construction of Amerongen weir |
| 1962-1970 | 891 | Construction of Driel weir |
| 2007-2018 | 867-970 | Room for the River measures |

**IJssel**

| Year | River km | Intervention |
|---|---|---|
| 1773-1782 | 878 | Modification of IJsselkop and nearby floodplain (pley) |
| 1850-1885 | 878-1005 | River training of IJssel |
| 1928 | 878-1005 | Narrowing: IJssel to 100 m |
| 1900-2002 | 878-975 | Dredging of sand and gravel. Only maintenance dredging for navigation since 2002 near the bifurcations. |
| 1954 | 904-909 | Bend cut-off in the IJssel near Doesburg (IJssel was 4.6 km shorter) |
| 1968-1969 | 891-895 | Bend cut-off in the IJssel near Rheden-De Steeg (IJssel was 4.0 km shorter) |
| 2007-2018 | 878-1005 | Room for the River measures |

**Niederrhein-Bovenrijn-Waal**

| Year | River km | Intervention |
|---|---|---|
| 1773-1782 | 867 | Modification of Pannerdense Kop and removal of bar at the mouth of PC. |
| 1850-1870 | 858-952 | Narrowing: Bovenrijn from 500 to 440 m and Waal to 500 to 360 m |
| 1870-1890 | 858-952 | Narrowing: Bovenrijn from 440 to 360 m and Waal to 360 to 310-320 m |
| 1900-1916 | 858-952 | Narrowing: Waal to 260 m upstream of Zaltbommel and 300 m downstream |
| 1900-2002 | 858-935 | Dredging of sand and gravel |
| 1985-1988 | 883-885 | Fixed bed installation at Nijmegen |
| 1985- | 665-860 | Sediment nourishment to mitigate bed level erosion at Niederrhein |
| 1994-1996 | 874-876 | Bendway weir installation at Erlecom |
| 1996-1999 | 925-928 | Fixed layer installation at St. Andries |
| 2007-2018 | 858-952 | Room for the River measures |
| 2014 | 858-861 | Fixed bed installation at Spijk |
| 2016 | 862-864 | Gravel nourishment at Lobith |
| 2019 | 862-864 | Gravel nourishment at Lobith |

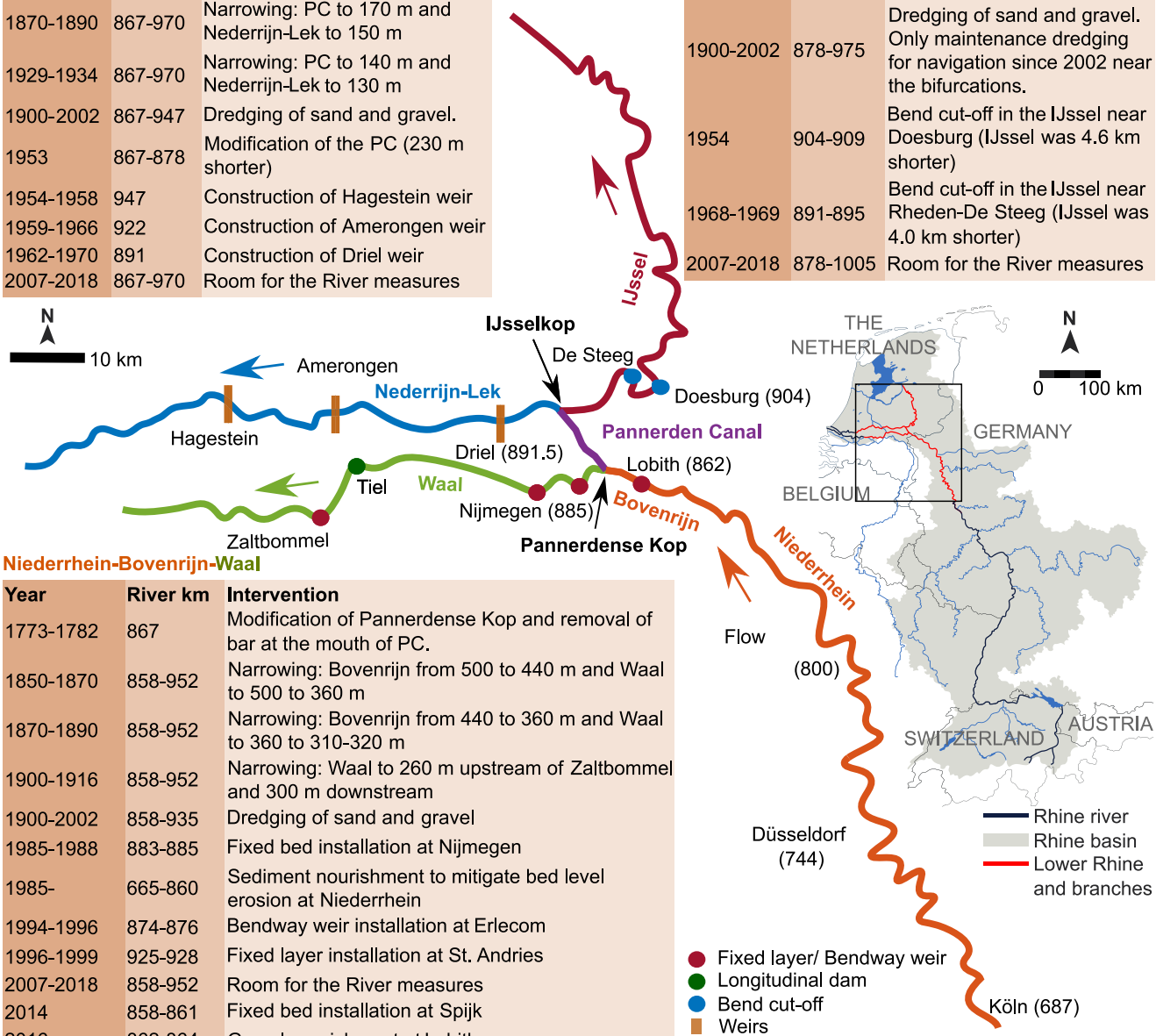


**Figure 1.** Human intervention in the bifurcation region of the upper Rhine delta since the 18th century. Numbers between parentheses indicate river km. Inset at the right-hand side shows the Rhine River basin.

between the Pannerden and IJsselkop bifurcations (river km 878.5) as the Pannerden Canal. Only the upstream 6 km of this reach was dug, and the downstream part is formally called the Nederrijn. At the IJsselkop bifurcation, the Pannerden Canal bifurcates into the Nederrijn and IJssel branches. The Waal is the widest and IJssel the narrowest of the bifurcates (Appendix A, Figure A1). At both bifurcations, the combined channel width of two bifurcates is larger than that of the upstream channel.

The bifurcation region is characterized by an extensive list of interventions (Figure 1, also see Ylla Arbós et al., 2021). Before 1700, the bifurcation apex was located 10 km upstream of its current location. It was moved to its current position by digging the Pannerden Canal in the early 1700s (Ten Brinke, 2005; Van de Ven, 1976). The Pannerden bifurcation developed as part of the Rhine network in the late Holocene, and the abandonment of the Nederrijn branch was the reason for digging the Pannerden Canal (Kleinhans et al., 2011). In the 18th century, the planform of the IJsselkop bifurcation was such that the IJssel branch took off from an inner bend. This configuration led to sediment deposition at the upstream IJssel, hampering navigation. In the late 1770s, the IJsselkop bifurcation was moved 1 km upstream, where it takes off from an outer bend, to prevent sediment deposition (Frings & Kleinhans, 2008; Schielen et al., 2007).

In the period between 1950 and 1970, three weirs were constructed in the Nederrijn-Lek branch (at Driel, Amerongen, and Hagestein, see Figure 1). The purpose of the Driel weir, in particular, is to control the flow partitioning at the IJsselkop bifurcation to maintain sufficient navigable depth in the IJssel branch and freshwater supply during low flows (Ten Brinke, 2005). Bends in the IJssel branch were cut off within the same period at Doesburg (in 1954) and De Steeg-Rheden (in 1969) for navigation purposes. These cut-offs led to a shortening of the IJssel branch by 8.6 km (Visser, 2000).

Fixed layers were constructed in outer bends of the bifurcation region at Nijmegen (1985) and Spijk (2014) and bendway weirs were placed at Erlecom (1996). Their purpose is to increase navigable width in sharp river bends (Havinga, 2020). Fixed layers and bendway weirs modify bend flow such that the inner bend deepens (Havinga, 2020).

In the Niederrhein, coarse sediment nourishments have been undertaken to mitigate channel bed erosion. In the period between 1991 and 2010, 8.4 Mt sediment (2 Mt fine gravel and 6.4 Mt coarse gravel and cobbles) was supplied with the largest quantities between river km 815–855 (Frings et al., 2014). Two sediment nourishment field tests were conducted in the Bovenrijn branch (river km 862–864) in 2016 and 2019 (Ylla Arbós et al., 2021).

Over the period 2007–2018, the intervention program "Room for the River" was conducted, focusing on increasing flood conveyance and nature restoration. Its extensive set of measures includes groyne and floodplain lowering, floodplain width increase, side-channel construction, channel bed deepening, and removal of obstacles (Havinga, 2020; Van Stokkom et al., 2005; Ylla Arbós et al., 2021).

The water discharge in the Lower Rhine is dominated by snow-glacier melt and rainfall (Pinter et al., 2006; Te Linde et al., 2010). At Lobith, the mean annual water discharge is approximately 2,210 $m^3/s$, and the mean annual peak flow is 6,540 $m^3/s$. Figures 2a and 2b show the Lobith hydrograph (data since 1901) and the associated flow duration curve. The highest discharge ever recorded at Lobith is 12,600 $m^3/s$ in 1926, and Figure 3 shows the 15 largest peak flow events since 1901 with recurrence period ranging from 4 to 120 years.

According to a treaty in the 18th century, the Waal, Pannerden Canal, Nederrijn, and IJssel branches, respectively, should receive approximately 2/3, 1/3, 2/9, and 1/9 of the Lobith discharge (Ferrand, 1847; Stumpe, 2009; Van de Ven, 1976). The Driel weir aims to maintain a minimum water discharge of 285 and 30 $m^3/s$ in IJssel and Nederrijn, respectively. For Lobith discharges smaller than 1,500 $m^3/s$, the priority is to maintain the 30 $m^3/s$ discharge in the Nederrijn (with the IJssel discharge sometimes being smaller than 285 $m^3/s$).

Bend sorting (Parker & Andrews, 1985) can be an important mechanism regarding sediment partitioning at a bifurcation. Secondary flow in a bend induces a near-bed sediment flux toward the inner bend, which deepens the outer bend relative to the inner bend. The associated transverse bed slope induces a component of the gravitational force down the transverse slope. The sum of the drag force (acting in the streamwise direction) and the transverse component of the gravitational force results in the fact that (a) coarse sediment is preferentially transported through the outer bend and finer sediment in the inner bend and (b) the bed surface sediment in the outer bend is coarser than in the inner bend (Parker & Andrews, 1985). With the Pannerden Canal and IJssel taking off from an outer bend of the upstream channel, bend sorting favors coarse sediment to be supplied to the Pannerden Canal and IJssel bifurcates (Frings & Kleinhans, 2008). As the bed surface grain size distribution is strongly related to the sediment flux (Blom et al., 2016; Blom, Arkesteijn, et al., 2017), the bed surface of the Pannerden Canal is coarser than the Waal. The bed surface of the upstream end of the IJssel is the coarsest among the bifurcates (Frings & Kleinhans, 2008).

The bed surface in the bifurcation region has coarsened over the past few decades (Ylla Arbós et al., 2021). This change in bed surface grain size is associated with the downstream migration of the Rhine gravel-sand transition (GST) and sediment nourishments in the German Rhine. Ylla Arbós et al. (2021) noted a significant advance (30–40 km) and flattening of the Rhine River GST: the length of the GST zone increased from about 50 km (river km 820–870) in

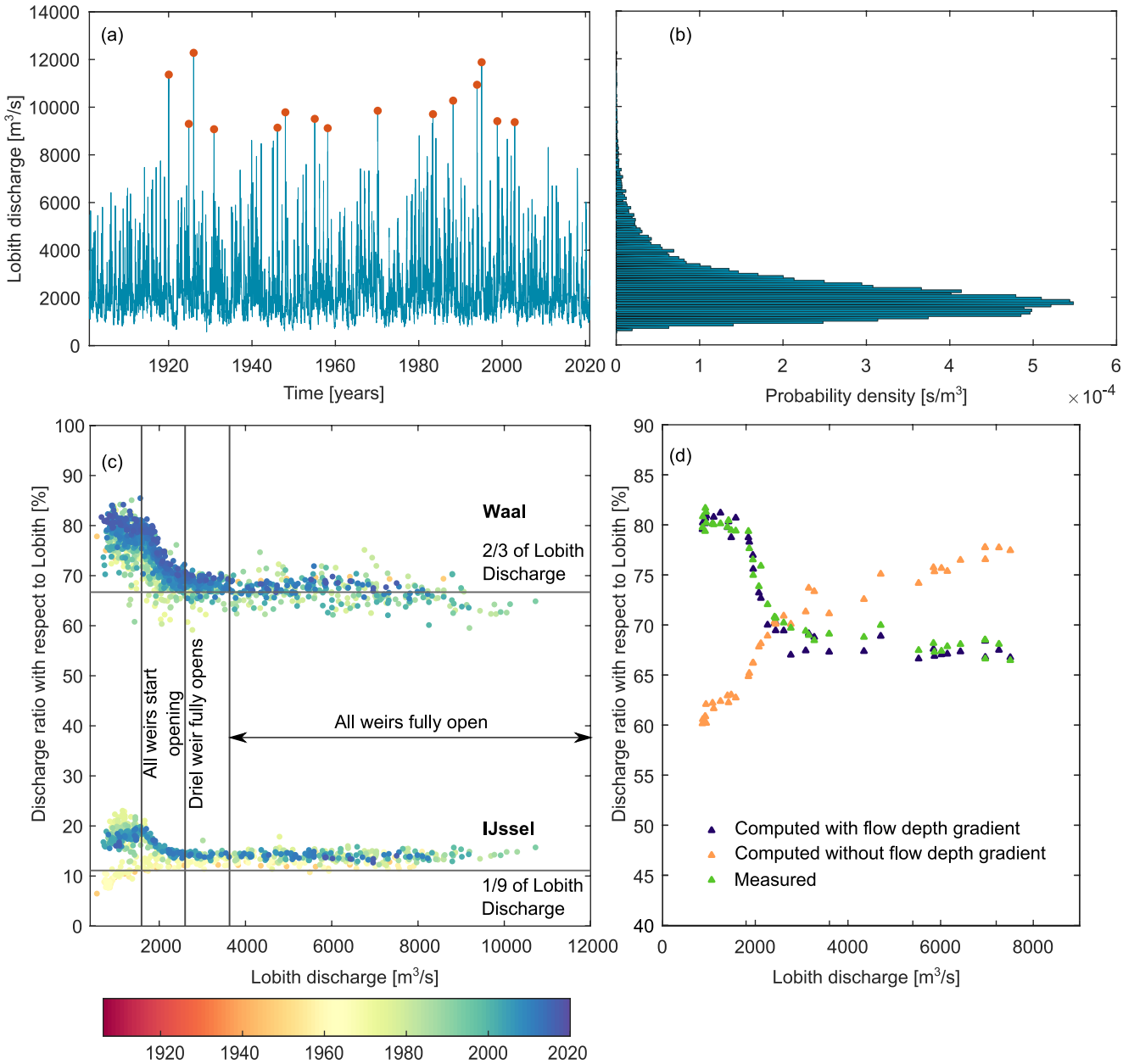


**Figure 2.** Water discharge characteristics in the bifurcation region: (a) measured water discharge at Lobith from 1901 to 2020 (source: Rijkswaterstaat); (b) associated flow duration curve at Lobith; (c) ratio of water discharge (measured using Ott current meter and Acoustic Doppler Current Profiler) at the upstream Waal and IJssel branches to the Lobith discharge; (d) ratio of measured and computed Waal discharge to measured Lobith discharge in 2017–2018. Orange dots in (a) indicate the peak flows shown in Figure 3. In (c) vertical lines indicate the 2016 weir opening program, and horizontal lines refer to the agreed flow partitioning according to a treaty in the 18th century, which states that the Waal and IJssel branches should receive approximately 2/3 and 1/9, respectively, of the Lobith discharge (Ferrand, 1847; Van de Ven, 1976).

1997 (Frings, 2011) to about 90 km (river km 840–930) in the Bovenrijn-Waal in 2020 (Ylla Arbós et al., 2021). The advance of a GST is a natural process (Blom, Chavarrías, et al., 2017), and advance of the Rhine River GST has likely been enhanced by the relatively coarse sediment nourishments in the Niederrhein (Ylla Arbós et al., 2021).

## 3. Partitioning of Water and Sediment Discharge

Under low flow conditions (i.e., a closed Driel weir), the Waal discharge is approximately 80% of the Lobith water discharge (Figure 2c). The weir at Driel is completely open for water levels at Lobith above

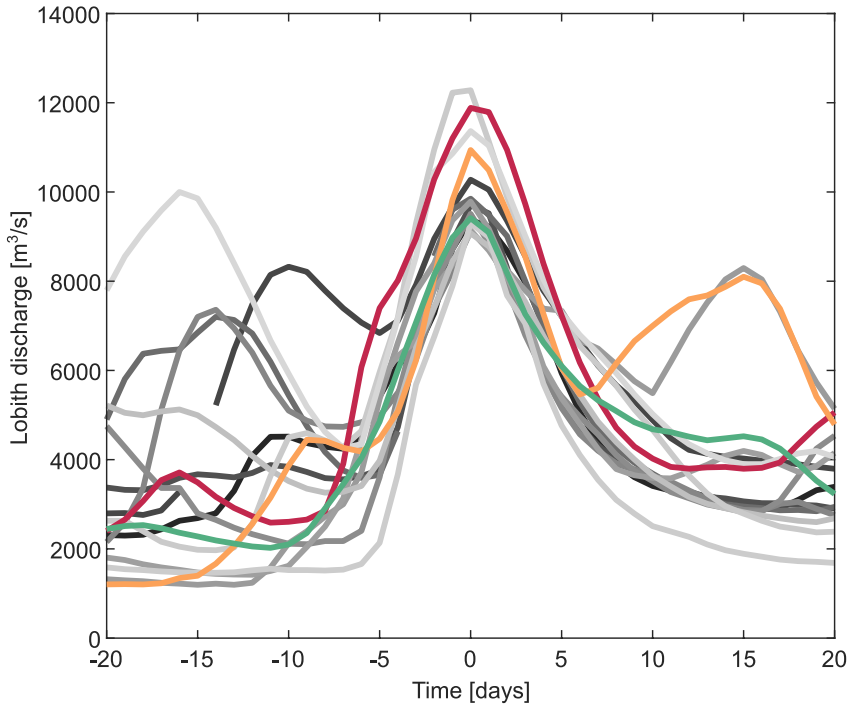


| Year | Date | Discharge ($m^3/s$) |
|---|---|---|
| 2003 | 06 January | 9372 |
| 1998 | 04 November | 9413 |
| 1995 | 31 January | 11885 |
| 1993 | 25 December | 10940 |
| 1988 | 30 March | 10274 |
| 1983 | 31 May | 9707 |
| 1970 | 27 February | 9850 |
| 1958 | 01 March | 9120 |
| 1955 | 21 January | 9510 |
| 1948 | 04 January | 9785 |
| 1946 | 12 February | 9140 |
| 1930 | 27 November | 9075 |
| 1926 | 04 January | 12600 |
| 1924 | 07 November | 9300 |
| 1920 | 18 January | 11365 |

**Figure 3.** Fifteen largest water discharges at Lobith since 1901. The table indicates the date and magnitude of the recorded peak of the waves.

10 m + NAP (where NAP denotes Normal Amsterdam Level), partially open for water levels between 8.60 m + NAP and 10 m + NAP, and fully closed for water levels below 8.60 m + NAP (Van Doornik et al., 2019). The relative Waal discharge under open weir conditions varies between 65% and 70% and decreases slightly for values of the Lobith discharge above 8,000 $m^3/s$. Figure 2c confirms that the Driel weir functions as its design was intended: the relative IJssel discharge increases at the expense of the Nederrijn when the weir is closed.

Backwater effects in the bifurcates can significantly affect the flow partitioning at a river bifurcation (Edmonds, 2012; Kleinhans et al., 2008, 2011). The Waal and Nederrijn-Lek flow out into the North sea, and the IJssel branch flows out into the IJsselmeer Lake. Backwater effects due to the North Sea and IJsselmeer Lake do not reach the bifurcation region (Figure 4). This does not imply that sea level and past changes in sea level do not affect the bifurcation region: current water level at the Pannerden bifurcation equals the sum of sea level and the integral of bifurcate channel slope times distance. The backwater effect due to the Driel weir does reach

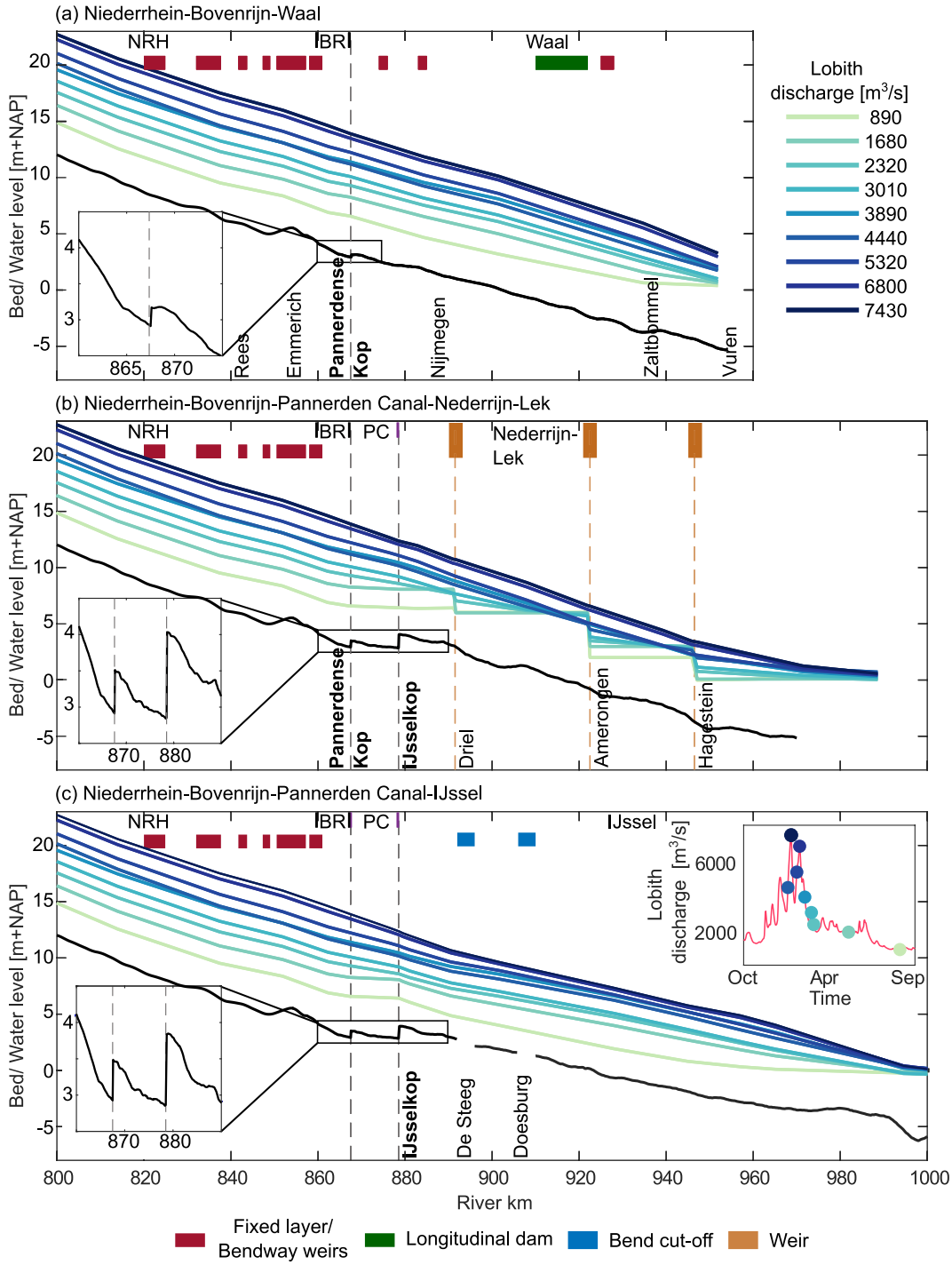


**Figure 4.** Water level (24 hr-averaged values) for various water discharge values at Lobith in 2017–2018 along the (a) Niederrhein (NRH)-Bovenrijn (BR)-Waal, (b) Niederrhein-Bovenrijn-Pannerden Canal (PC)-Nederrijn-Lek, and (c) Niederrhein-Bovenrijn-Pannerden Canal-IJssel. The right inset in (c) shows the 2017–2018 Lobith hydrograph. Bed level (black line) in the Niederrhein and the Dutch reaches corresponds to bathymetric surveys of years 2010 and 2020, respectively. Left insets show the bed steps at the bifurcations. Sources of water level data are Rijkswaterstaat and German Federal Waterways and Shipping Administration (WSV).

both bifurcations (Figure 4b) increasing the relative water discharge in the Waal and IJssel during low flow rates (Figure 2c). Pannerden Canal is governed by two opposing backwater effects: the Driel weir causes a streamwise increase in flow depth and the backwater due to the IJsselkop bifurcation leads to a streamwise decrease in flow depth. The latter is due to the fact that the IJssel water level is low relative to the Nederrijn. During low flows,

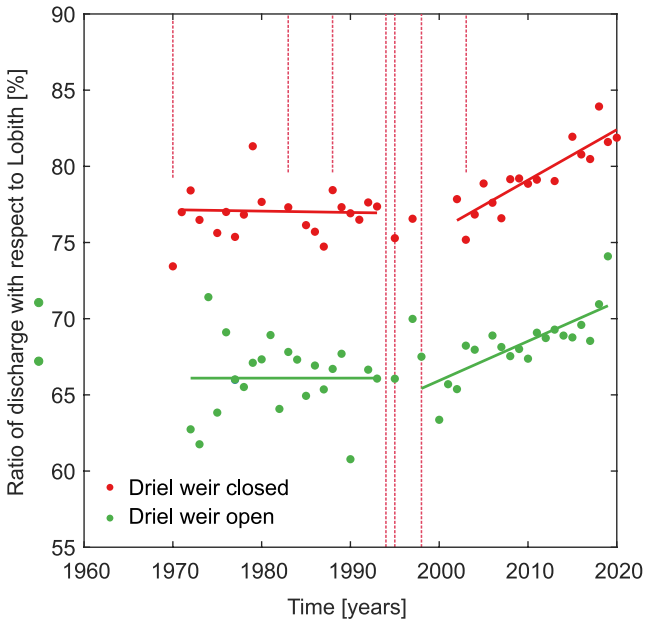


**Figure 5.** Ratio of Waal to Lobith water discharge as a function of time. The green dots outside the time axis indicate the measurements of Brunings in 1790–1792 (Hesselink et al., 2006). Red dotted lines at the top indicate the peak flows indicated in Figure 3, with the 1993–1995–1998 peak flows extending downward.

the Driel weir backwater dominates and flow depth in the Pannerden Canal increases in the streamwise direction. During peak flows, the Driel weir is lifted, and the only backwater effect is the one due to the IJsselkop bifurcation. This means that during peak flows, the flow depth over the Pannerden Canal decreases with streamwise position (Figure 4b), and the flow spatially accelerates.

We compute the annual mean flow partitioning ratio based on measurements using Ott current meters and Acoustic Doppler Current Profiler (ADCP) (Figure 5). We refer to Appendix A for details on discharge measurements and data analysis. We distinguish between two discharge regimes to assess whether the flow partitioning shows any temporal trend: (a) a low flow regime in which the Driel weir is fully closed ($Q_{Lobith} < 1{,}500$ m$^3$/s where $Q_{Lobith}$ denotes the Lobith water discharge), and (b) a high flow regime in which the Driel weir is entirely open ($Q_{Lobith} > 2{,}500$ m$^3$/s). For both discharge regimes, the ratio of Waal to Lobith water discharge was stable between 1970 and the early 1990s, and has increased since the peak flows of 1993–1995–1998 by 0.2%–0.4% per year (Figure 5). Text S1 in Supporting Information S1 shows various fits to the time series of the Waal fraction of the Lobith discharge: (a) a moving average window (window size of 20 years), (b) the Loess method (Cleveland, 1979) (with data span equal to 0.6), and (c) a piecewise linear regression with imposed breakpoints at 1993 and 1998. The data are characterized by significant scatter to which the Loess method is relatively sensitive, as it requires a dense data set (Text S1 in Supporting Information S1). The moving average and Loess methods confirm a breakpoint around the 1993–1995–1998 peak flows. For the flow partitioning in the intermediate regime where the Driel weir is partially closed, we refer to the Text S2 in Supporting Information S1.

There have been limited field studies (in 1998, 2002, and 2004) measuring the sediment flux and its partitioning over the bifurcates (Frings & Kleinhans, 2008; Frings et al., 2015, 2019; Kleinhans et al., 2007). The uncertainty associated with these data ranges between 40% and 100%. Table 1 compares the sediment partitioning over the branches with the associated flow partitioning. The relative sand flux received by the Waal branch is significantly larger than its share of the Lobith discharge. This is because of bend sorting (Section 2). Immediately upstream of the Pannerden bifurcation, the near-bed sand flux is directed toward the inner bend and, as a result, to the Waal branch (Frings & Kleinhans, 2008; Parker & Andrews, 1985). The partitioning of the clay-silt fraction was assumed to be equal to the flow partitioning (Frings et al., 2019). For the other grain size classes, the IJssel fractions of the Lobith sediment fluxes are significantly smaller than its share of the Lobith discharge. This is because both the Pannerden Canal and IJssel branches take off from an outer bend, which reduces their sediment flux.

**Table 1**
*Flow and Sediment Partitioning at the Pannerden and IJsselkop Bifurcations, Expressed as Water Discharge Relative to Associated Lobith Discharge and Grain-Size Specific Annual Sediment Fluxes Relative to Associated Lobith Fluxes*

| | Relative water discharge | Clay and silt <0.063 mm | Sand 0.063–2 mm | Fine gravel 2–16 mm | Coarse gravel 16–63 mm |
|---|---|---|---|---|---|
| Waal | 68%–70% | 70% | 88% | 65% | 75% |
| IJssel | 13%–14% | 15% | 7% | 7% | 6% |

*Note.* Sediment partitioning is based on Frings et al. (2015, 2019). Uncertainty regarding sediment fluxes ranges between 40% and 100%. Flow partitioning values relate to open Driel weir conditions.

## 4. Spatial and Temporal Change in Bed Level

Over the last century, the entire domain of the Lower Rhine has undergone channel incision (Figure 6). The region of the Pannerden bifurcation (from roughly 5 km upstream down to 10–15 km downstream) has eroded by 2–3 m, about twice as much as the surrounding area. For the Waal branch, the total amount of erosion gradually decreases with streamwise position, which reflects a gradual channel slope decrease or channel tilting (Figure 6a). The total amount of erosion is the largest over the Pannerden Canal (Figure 6b).

A bifurcation is typically associated with a discontinuity in bed level (see insets of Figures 4 and 7). Such a bed step equals the difference in flow depth between the upstream branch and downstream branch, as water level, by definition, is continuous. The difference between the upstream and downstream flow depth results from the change in water discharge and channel width over the bifurcation (Asmerom, 2001; Kleinhans et al., 2013). The Waal bed step

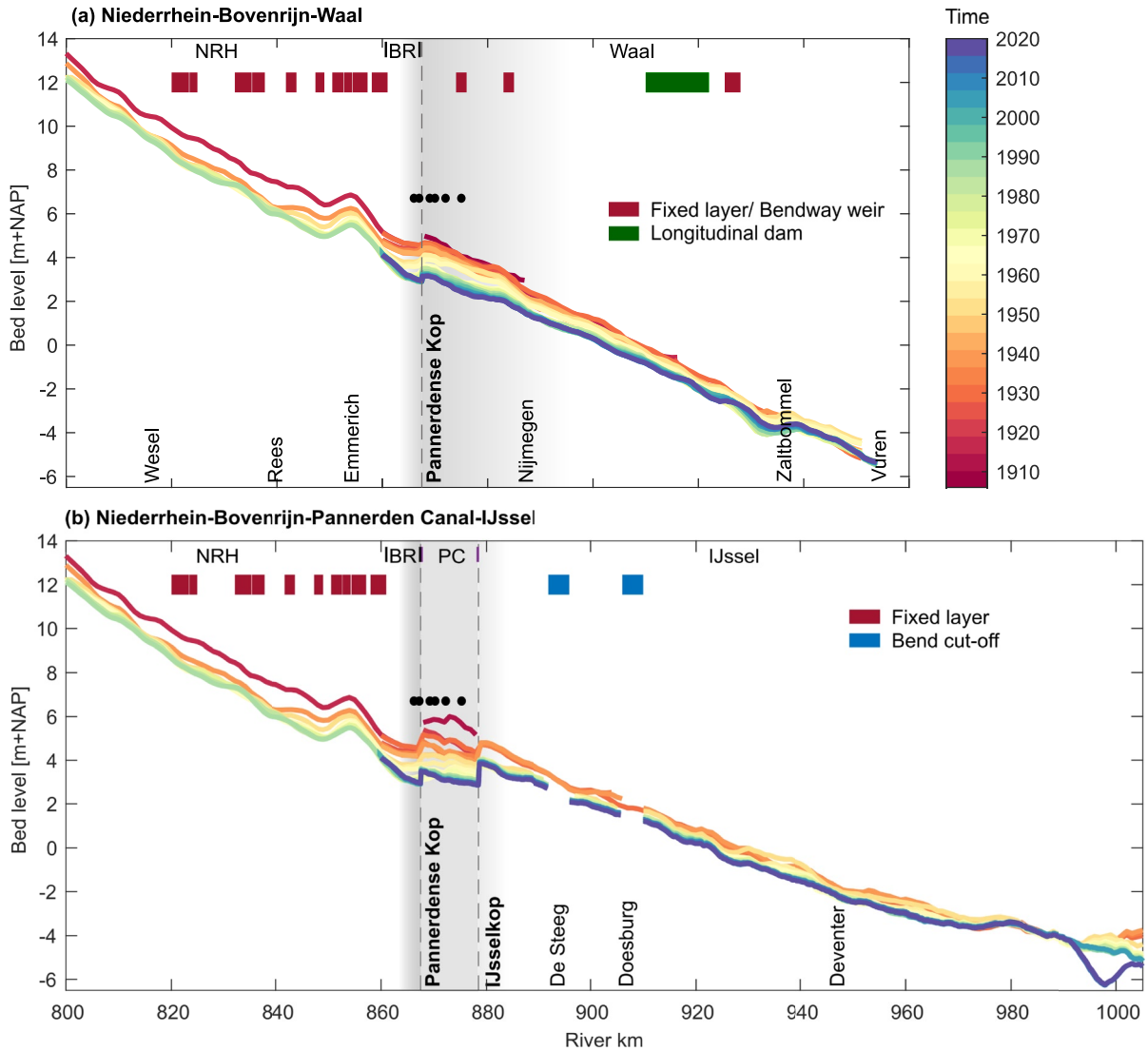


**Figure 6.** Bed level in (a) Niederrhein (NRH)-Bovenrijn (BR)-Waal, and (b) Niederrhein-Bovenrijn-Pannerden Canal (PC)-IJssel branches over the past century. The shaded areas indicate zones of intense erosion. The black dots indicate the locations for which temporal change in bed level is shown in Figure 7.

is smaller than the other bed steps in the bifurcation region. The difference in bed level between the bifurcates (i.e., the inlet step) yields a transverse bed slope upstream of the bifurcation that leads to a transverse flux of bed material load to the deeper bifurcate due to gravity (Bolla Pittaluga et al., 2003; Kleinhans et al., 2013).

We hypothesize that the break in the flow partitioning trend observed in Figure 5 is due to sediment deposition in parts of the bifurcation region resulting from a rapid succession of peak flows. To test this hypothesis, we analyze the temporal change of bed level in the bifurcation region and assess whether bed level shows a sudden temporal change. To this end, we look into the time variation of bed level at various positions (at 0.5, 1.5, 4.5, and 7.5 km) upstream and downstream of the Pannerden bifurcation (Figure 7).

Figures 7a and 7b illustrate that the rapid succession of the 1993–1995–1998 peak flows have caused sediment to deposit over the upstream part of the Pannerden Canal. In other words, during these peak flows the sediment supply into the Pannerden Canal exceeded its sediment transport capacity. Data uncertainty complicates attributing the changes to one, two or all of the 1993–1995–1998 peak flows. The Bovenrijn bed level right upstream of the Pannerden bifurcation decreased following the peak flows (Figure 7a).

Prior to the 1993–1995–1998 peak flows, the erosion rate in the upstream Pannerden Canal was slightly larger than the upstream Waal (Figure 7). Besides sudden deposition, the 1993–1995–1998 peak flows led to a decrease

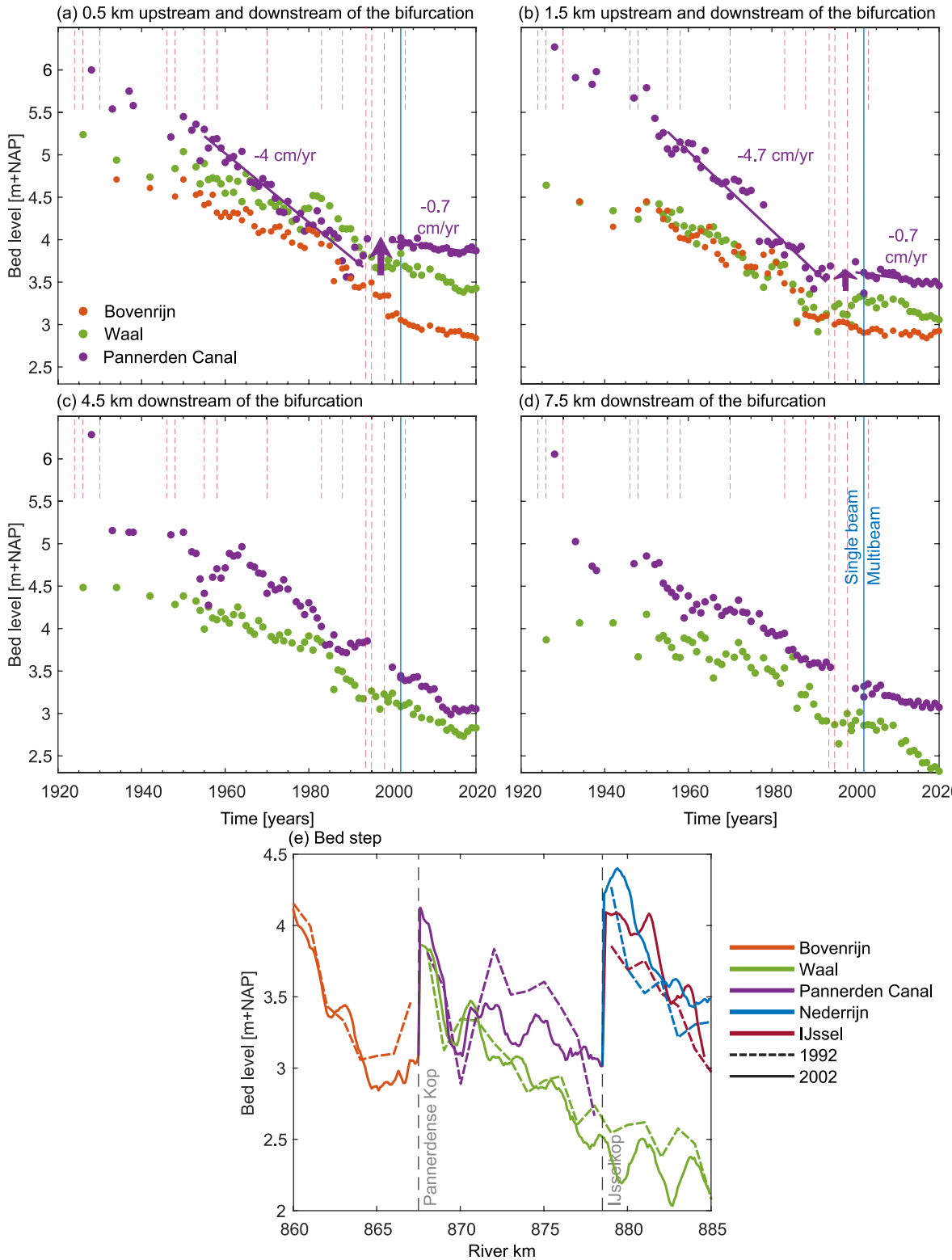


**Figure 7.** Bed level as a function of time at (a) 0.5 km upstream (river km 867) and downstream of the Pannerden bifurcation (river km 868), (b) 1.5 km upstream (river km 866) and downstream (river km 869) of the Pannerden bifurcation, (c) 4.5 km downstream of the Pannerden bifurcation (river km 872), and (d) 7.5 km downstream of the Pannerden bifurcation (river km 875). Subplot (e) shows bed steps in 1992 and 2002. Linear fits in (a) and (b) were applied to Pannerden Canal bed level data for the periods 1960–1993 and 1998–2020 to indicate the bed level discontinuity. Here, bed level data are averaged over 1 km. Red dotted lines at the top indicate the peak flows indicated in Figure 3, with the 1993–1995–1998 peak flows extending downward.

of the erosion rate in the upstream Pannerden Canal. Since these peak flows, the upstream Waal has eroded at a larger rate than the upstream Pannerden Canal.

The rapid aggradation in the upstream Pannerden Canal (Figure 7a) followed by an ever-increasing Waal share of the Lobith discharge (Figure 5) and differential erosion rate between the Waal and Pannerden Canal (Figure 7) seems to have not occurred for the other peak flows shown in Figure 3.

The upstream Waal eroding faster than the upstream Pannerden Canal co-occurs with the continued change of the flow partitioning at the Pannerden bifurcation (Figure 5). The fact that a differential erosion rate of the upstream bifurcates is associated with a continued change of the flow partitioning can be understood from the one-dimensional conservation equations for flow (Saint Venant, 1871). Under stationary conditions, the Saint Venant equations reduce to the backwater equation $S_d = (S - S_f)/(1 - Fr^2)$, where $S_d$ denotes the streamwise gradient of flow depth $H$ ($S_d = dH/dx$), $S$ is the channel bed slope, $Fr$ is the Froude number, and $S_f$ is the friction slope ($S_f = c_f Fr^2$ where $c_f$ is the non-dimensional friction coefficient). Replacing $Fr^2$ by $Q_w^2/\left(gB^2H^3\right)$ (where $Q_w$ denotes the water discharge, $g$ the acceleration due to gravity, and $B$ the channel width), the backwater equation for a compound channel takes the following form:

$$Q_{wi} = B_i\sqrt{gH_i^3\,\frac{S - S_{di}}{c_{fi} - S_{di}}} \tag{1}$$

where subscript $i$ denotes one of the three compartments of a compound channel: main channel, groyne field, or floodplain. The water discharge integrated over a cross-section then becomes $Q_w = \sum_{i=1}^{3} Q_{wi}$. The faster erosion rate for the upstream Waal increases the flow depth $H$ relative to the one in the upstream Pannerden Canal because of water level continuity over the Pannerden bifurcation. As a result, a differential erosion rate (Figure 7) is accompanied by a continued change in flow partitioning (Figure 5).

Equation 1 also illustrates the importance of backwater effects in the bifurcates regarding the flow partitioning at a bifurcation. As described in Section 3, the backwater effects in the Pannerden Canal stem from two opposing effects: the Driel weir (only during low flows) and the IJsselkop bifurcation (see Text S3 in Supporting Information S1). We apply Equation 1 to the 2018 hydrograph in Figure 4c to assess the importance of backwater effects in the Pannerden Canal. We compare the Waal discharge (here taken as Lobith discharge minus the Pannerden Canal discharge) using Equation 1 with and without accounting for the flow depth gradient $S_d$ in the Pannerden Canal (Figure 2d). We use a $c_f$ value of 0.004 for the main channel corresponding to a Chézy friction coefficient of 50 $m^{1/2}/s$ (Sloff & Mosselman, 2012). We assume the groyne field and floodplain to be rougher than the main channel and adopt a $c_f$ value equal to 0.010 (Chézy friction coefficient of 30 $m^{1/2}/s$). Total water discharge appears to be insensitive to the latter friction value, as the groyne fields and floodplain do not significantly contribute to flood conveyance under these conditions. Strictly speaking, the assumption that the $c_f$ value does not depend on the flow rate is not realistic, as form drag due to bedforms varies with the flow rate. Here, however, the assumption of a constant $c_f$ value suffices as a first estimate to assess the relative importance of backwater effects on the flow partitioning. Figure 2d shows a match between the computed and measured Waal fraction of the Lobith discharge when accounting for the flow depth gradient in the Pannerden Canal, $S_d$. This confirms the large role of backwater effects in the bifurcates regarding flow partitioning at a bifurcation.

The rapid succession of peak flows also caused sudden sediment deposition immediately downstream of the IJsselkop bifurcation in both the Nederrijn and IJssel bifurcates (Text S4 in Supporting Information S1). Here, both upstream bifurcates aggraded with a similar magnitude, which may have stabilized the flow partitioning at the IJsselkop (Figure S4 in Supporting Information S1).

In summary, our analysis shows that the rapid succession of two to three peak flows has caused sudden sediment deposition over the upstream part of the Pannerden Canal. This has resulted in a breakpoint in both the flow partitioning and the relative erosion rate over the upstream part of the bifurcates. More specifically, the sudden aggradation in the upstream Pannerden Canal has resulted in (a) the Waal fraction of the Lobith discharge gradually increasing with time ever since and (b) the upstream Waal eroding faster than the upstream Pannerden Canal. The latter two effects logically co-occur, as explained above.

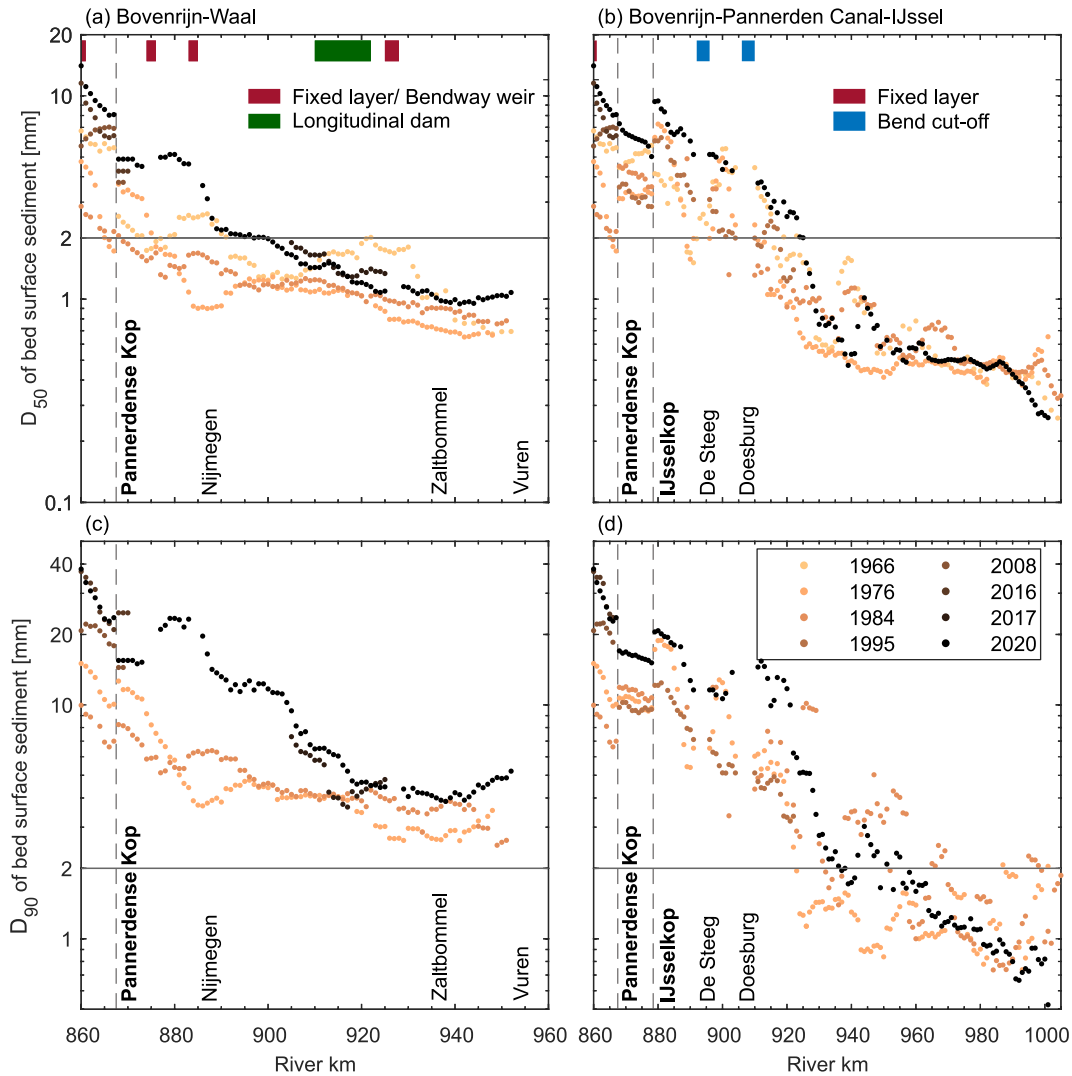


**Figure 8.** The 50th and 90th percentiles of width-averaged bed surface grain size ($D_{50}$ and $D_{90}$): (a) $D_{50}$ at Bovenrijn-Waal, (b) $D_{50}$ at Bovenrijn-Pannerden Canal-IJssel, (c) $D_{90}$ at Bovenrijn-Waal, and (d) $D_{90}$ at Bovenrijn-Pannerden Canal-IJssel. Bed surface grain size is averaged over a window of 10 km.

## 5. Change in Bed Surface Grain Size

During peak flows, the bed surface and subsurface sediment is reworked through dune migration and dune sorting (Blom, 2008; Blom & Parker, 2004; Blom et al., 2003; Kleinhans, 2001, 2005). A flood wave may form a coarse layer at the base of dunes and leave a remnant gravel layer, and subsequent peak flows may rework remnants of previous years (Blom et al., 2003; Kleinhans, 2001, 2005). Our current analysis does not shed light on these dynamics, as the temporal density of bed surface grain size data is insufficient. We are, however, able to assess changes in bed surface grain size over a longer time scale. Over recent decades the bed surface sediment of the Rhine branches has coarsened (Frings, 2011; Frings et al., 2009; Ten Brinke, 1997; Ylla Arbós et al., 2021). In addition, Ylla Arbós et al. (2021) pointed at the downstream advance of Rhine River GST (Section 2). The coarsening of the channel bed surface has been attributed to the natural migration of the GST and coarse sediment nourishments in the German Rhine (Blom, Chavarrías, et al., 2017; Ylla Arbós et al., 2021). This temporal bed surface coarsening in the Rhine River originates from at least 900 years ago (Frings et al., 2009).

Here we focus on the change in channel bed grain size within the bifurcation region, and compare width-averaged 50th and 90th percentiles of grain size ($D_{50}$ and $D_{90}$, respectively) of the bed surface sediment (Figure 8). The channel bed surface is a mobile armor, which compensates for the mobility difference between coarse and fine

sediment by allowing for sufficient transport capacity of the coarse sediment (Blom et al., 2016; Parker & Klingeman, 1982; Parker & Sutherland, 1990). Presence of a mobile armor is reflected by the fact that the bed surface sediment is coarser than the subsurface sediment. This holds particularly for the Pannerden Canal and IJssel branches (Gruijters et al., 2001, 2003). Since the late 1990s, the bed surface within the bifurcation region has coarsened (Figure 8). Bed surface coarsening suggests temporal coarsening of the sediment supply from upstream, as the bed surface grain size distribution is strongly related to the grain size distribution of the sediment flux (Blom, Arkesteijn, et al., 2017; Blom et al., 2016; Parker & Toro-Escobar, 2002). Width-averaged 50th and 90th percentiles of grain size of the bed surface sediment for the Pannerden Canal-Nederrijn-Lek are provided in the Text S5 in Supporting Information S1.

The authors believe that the bed surface coarsening within the bifurcation region and associated temporal coarsening of the sediment flux may explain (a) the sudden sediment deposition at the upstream Pannerden Canal associated with the rapid succession of peak flows (1993–1995–1998), as bend sorting upstream of the Pannerden bifurcation provides a coarser sediment supply to the Pannerden Canal, and (b) the bifurcation region showing a reduced erosion rate following the rapid succession of peak flows. We will elaborate on this in Section 7.

## 6. Sediment Supply Versus Sediment Transport Capacity

A bifurcation can be considered the upstream boundary for water and sediment discharge of the downstream bifurcates (Bolla Pittaluga et al., 2003; Schielen & Blom, 2018; Wang et al., 1995). Over the upstream part of each bifurcate, the variable flow rate induces an upstream boundary segment (An, Cui, et al., 2017; An, Fu, et al., 2017; Arkesteijn et al., 2019, 2021; Blom, Arkesteijn, et al., 2017). In an upstream boundary segment (sometimes called hydrograph boundary layer), the instantaneous difference between the sediment supply from upstream and the sediment transport capacity leads to the formation of downstream migrating adjustment waves regarding bed level and bed surface grain size. The adjustment waves tend to (but not necessarily) diffuse while they migrate downstream, and therefore they are typically limited to a certain distance (An, Cui, et al., 2017; An, Fu, et al., 2017). Here we determine the 5-year averaged (moving window) aggradation rates since 1960 to assess whether such adjustment waves originate at the two bifurcations (Figure 9).

Each peak flow in Figure 3 seems to initiate a downstream migrating erosion wave originating at the Pannerden bifurcation down the Waal branch (white lines in Figure 9). An erosion wave implies that, during peak flows, the sediment transport capacity of the Waal exceeds the sediment supply from upstream. The sediment supply to each of the bifurcates depends on the grainsize-specific sediment partitioning at the bifurcation. We hypothesize that the behavior of adjustment waves along the Waal branch is associated with it being relatively narrow given its water discharge.

Earlier adjustment waves seem to migrate faster than more recent waves (Figure 3). This temporal decrease of the migration celerity seems to be related to the temporal coarsening of the sediment flux and bed surface sediment (Figure 8). This hypothesis can be tested using a simple analysis using the conservation equations of water mass, streamwise momentum, and sediment continuity (Exner, 1920) using the sediment transport relation of Engelund and Hansen (1967). In such a case, the celerity of a bed level disturbance is proportional to the sediment transport rate per unit width. As the sediment transport rate is inversely related to the median grain size (Engelund & Hansen, 1967), bed surface coarsening can indeed reduce the celerity of bed disturbances (see Jansen et al. (1979) for a detailed analysis).

Some of the adjustment waves in Figure 9 may originate from further upstream (e.g., in the Niederrhein), but the limited temporal resolution of the Niederrhein data does not allow for such verification. The numerous engineering interventions in the system induce adjustment waves, as well (e.g., the downstream migrating waves originating at the fixed layers at Nijmegen and St. Andries in the Waal branch). The dredging in the 1980s (Visser, 2000) has led to intense erosion over the Bovenrijn and Waal branches. Information on the aggradation rate for other branches is provided in the Text S6 of Supporting Information S1. Celerity of the downstream migrating waves along the Waal ranges between 0.6 and 1.7 km/yr, Pannerden Canal between 0.7 and 1.4 km/yr, Nederrijn between 0.5 and 1.2 km/yr, and IJssel between 0.7 and 0.9 km/yr. It can be expected that the engineering interventions have also led to upstream migrating adjustment waves, but these cannot be clearly distinguished.

Figure 10 shows a conceptual representation of sediment supply versus sediment transport capacity at the upstream end of the bifurcates and associated bed level change during mean flow and peak flows. The balance

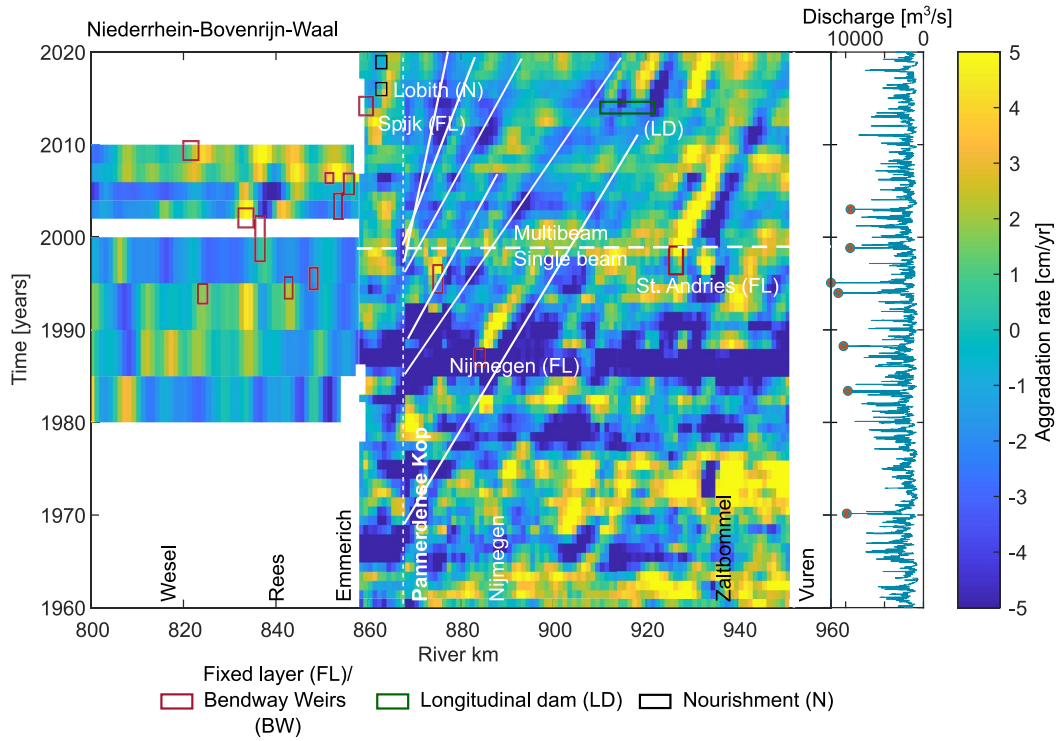


**Figure 9.** Five-year averaged aggradation rates for Niederrhein-Bovenrijn-Waal. The right-hand side shows the associated time series of Lobith water discharge. Dots in the hydrograph indicate the peak flows of Figure 3. The white lines indicate downstream migrating erosion waves initiated at the Pannerden bifurcation for peak flows after 1960 listed in Figure 3. The aggradation rate is determined based on a 2-km moving average window.

of sediment supply versus sediment transport capacity under mean flow conditions is based on annual sediment flux data (Frings et al., 2015). The balance of sediment supply versus sediment transport capacity under peak flow conditions (Figure 10) is based on the assumptions that (a) both the sediment supply and sediment transport capacity increase relative to the above mean flow conditions, and (b) for all branches except for the Waal, the sediment supply increases more strongly than the sediment transport capacity, which matches bed level change resulting from the rapid succession of the 1993–1995–1998 peak flows (see Figure 7 and Figure S4b in Supporting Information S1).

## 7. Discussion

The relative increase of the Waal discharge feeds back on the larger-scale river dynamics. The sediment supply to the Waal bifurcate does not sufficiently increase with its increasing flow rate during peak flows. This mismatch between sediment supply and sediment transport capacity further increases its relative fraction of the Lobith water discharge. The changing flow partitioning may continue to decrease the equilibrium channel slope for the Waal branch. The associated decrease of the Waal channel slope adds to the ongoing river response (i.e., slope decrease and associated channel bed erosion) to past training works and channel narrowing.

The current development of the Pannerden bifurcation indicates that it is in an unstable situation where one branch (the Waal) grows at the expense of the other branch (the Pannerden Canal). Without interventions, this may eventually lead to the abandonment of the Pannerden Canal (Kleinhans et al., 2013; Schielen & Blom, 2018; Wang et al., 1995).

Other peak flows in Figure 3 seem to have induced a different system response than the rapid succession of the 1993–1995–1998 peak flows. Researchers have defined thresholds for peak flows to initiate certain channel response, for instance thresholds related to peak flow magnitude, peak flow frequency (Lisenby et al., 2017), peak flow duration (Gervasi et al., 2021), streampower (Magilligan, 1992; Yochum et al., 2017), and sediment

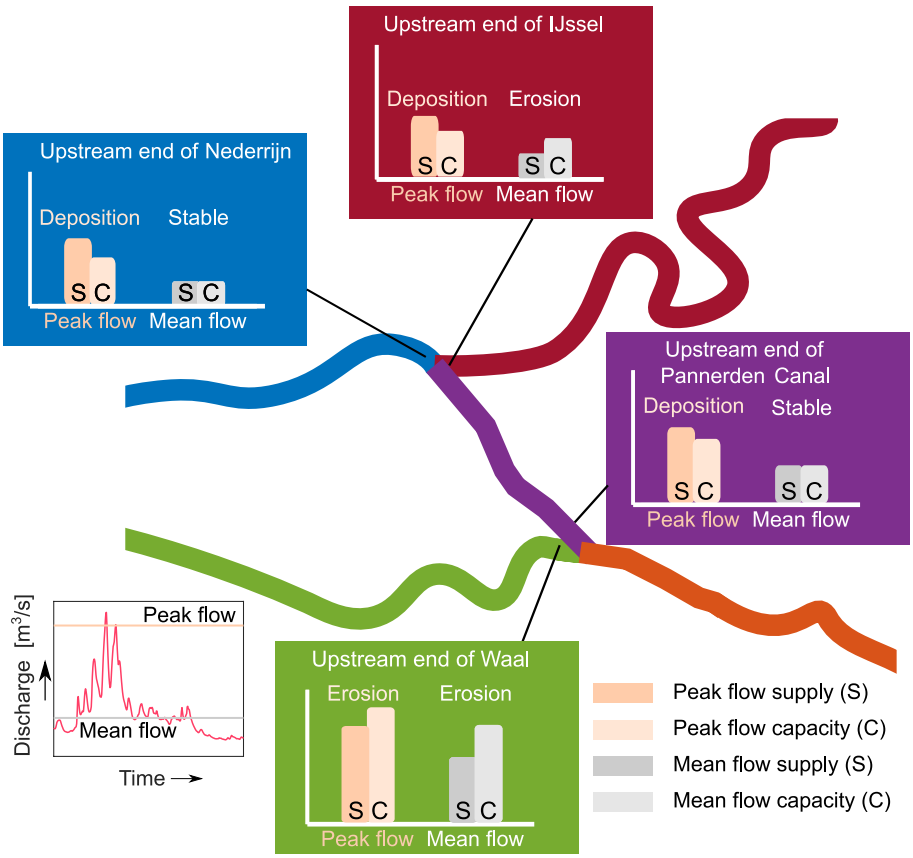


**Figure 10.** Conceptual representation of sediment supply and sediment transport capacity at the upstream part of the bifurcates and associated bed level change during mean and peak flow conditions.

flux volume (East et al., 2018; Lisenby et al., 2017). However, the significance of these thresholds and their relative role during peak flows are not generically valid and often unclear.

We come up with three possible explanations on why the system response to the 1993–1995–1998 peak flows seems to have been different from other peak flows. The first explanation concerns the role of the quick succession or net duration of the peak flow events. The rapid succession of peak flows may have resulted in insufficient time for the flow to disperse deposited sediment during inter-flood periods. Our second explanation relates to the temporal coarsening of the sediment flux and bed surface sediment in the bifurcation region. This temporal coarsening of the sediment flux together with bend sorting right upstream of the Pannerden bifurcation may have resulted in an increased coarse sediment supply to the upstream Pannerden Canal branch, which led to sediment deposition due to insufficient sediment transport capacity. The third explanation relates to both phenomena (hypotheses 1 and 2) co-occurring. The explanations will be investigated in future research.

Sudden channel bed aggradation during peak flows, as observed during the peak flows of 1993–1995–1998, is not accounted for in current flood risk management, and may increase flood risk beyond expected levels. Furthermore, the subsequent slow change of the flow partitioning affects flood risk in the bifurcates. In addition, the gradually decreasing flow in one bifurcate may increasingly hinder freshwater supply and navigability during low flow conditions.

Flow and sediment partitioning at a bifurcation are influenced by the upstream hydrograph and downstream base level, both of which will change in the future due to climate change. Currently, peak flows and interventions dominate the bifurcation response over sea level rise (SLR). In the future, the impact of SLR on the bifurcation region will increase through backwater effects and associated upstream-migrating bed level adjustment. However, we expect that the increased probability of extreme precipitation and flow events associated with climate change (Klein Tank et al., 2014; Sperna Weiland et al., 2015) will affect the bifurcation region more strongly than SLR

(Ylla Arbós et al., 2023). In addition, the sediment supply from the Niederrhein may coarsen further. As a result, we anticipate that more frequent and extremer peak flow events, maybe in combination with a coarser sediment supply, will impact the bifurcation dynamics, resulting in possibly accelerated change of the flow partitioning at the Pannerden bifurcation. These effects will be addressed in our future work.

River bifurcations are present in almost every medium-size and large river around the world with different levels of engineering: the Mezcalapa-Samaria-Carrizal system in Mexico (Mendoza et al., 2019, 2021), Ganga-Padma–Hooghly system in India (Gupta et al., 2014), the Bala-Lower Old Danube system in Romania (Yossef et al., 2016), and the Mississippi-Atchafalaya system in the USA (Edmonds, 2012). Planform, geometry, sediment characteristics, hydrograph, and interventions vary among them. For example, sediment retention and homogenization of the hydrograph due to upstream dams influence the flow partitioning at the Mezcalapa river bifurcation (Mendoza et al., 2021), the Farakka Barrage in the Ganga-Padma system affects the flow partitioning at the bifurcation upstream of Hooghly river (Gupta et al., 2014), and the Old River Control Structure determines the flow partitioning at the Mississippi-Atchafalaya bifurcation (Edmonds, 2012). Long-term observations of flow partitioning and bed level dynamics will be required to understand how these different bifurcations respond to peak flows and climate change.

## 8. Conclusions

Semi-centennial observations in the bifurcation region in the engineered upper Rhine delta have shown that the Waal bifurcate takes an increasing fraction of the upstream water discharge at the expense of the other bifurcate (Pannerden Canal).

The gradual increase of the Waal discharge co-occurs with the Waal channel eroding faster than the Pannerden Canal bifurcate.

Both these gradual changes are possibly triggered by the rapid succession of two to three peak flows (1993, 1995, and 1998).

The rapid succession of the 1993–1995–1998 peak flows resulted in sudden sediment deposition over the upstream part of the bifurcate that is subsequently characterized by a gradually decreasing fraction of the upstream channel's water discharge. This sudden sediment deposition and associated bed level increase seem to have triggered the above changes in flow partitioning and relative erosion rates.

The system response to the 1993–1995–1998 peak flows seems to have been different from other peak flows, which we believe to be due to the quick succession or net duration of the peak flows (resulting in insufficient time to disperse the deposited sediment during inter-flood periods) and the temporal coarsening of the sediment flux and bed surface sediment.

The temporal bed surface coarsening seems to be due to a temporal coarsening of the sediment supply from upstream, as the two have been shown to be strongly related. The bed surface coarsening has likely reduced the celerity of the downstream migrating adjustment waves that originate at the bifurcation.

It is generally assumed that peak flows do not lead to significant bed level change due to (a) the difference in timescale between peak flows and bed level change, and (b) the limited probability of peak flows (i.e., their limited share in the flow duration curve). Our findings illustrate that peak flows can play a large role through sudden and local sediment deposition that may trigger a slow change in flow partitioning and bed level among the bifurcates.

## Appendix A: Methods

Our analysis is based on field data on bed level, bed surface grain size, water level, and water discharge. Some data sets span over a century. Logically there have been several temporal changes in measurement techniques (e.g., single-beam to multibeam echo sounders for bed level). In addition, as the Rhine River spans across borders, techniques also vary spatially. Such temporal and spatial changes in measurement techniques increase the uncertainties in the measured data. Details on bed level and bed surface texture data collection and treatment used in this study can be found in the Supporting Information of Ylla Arbós et al. (2021).

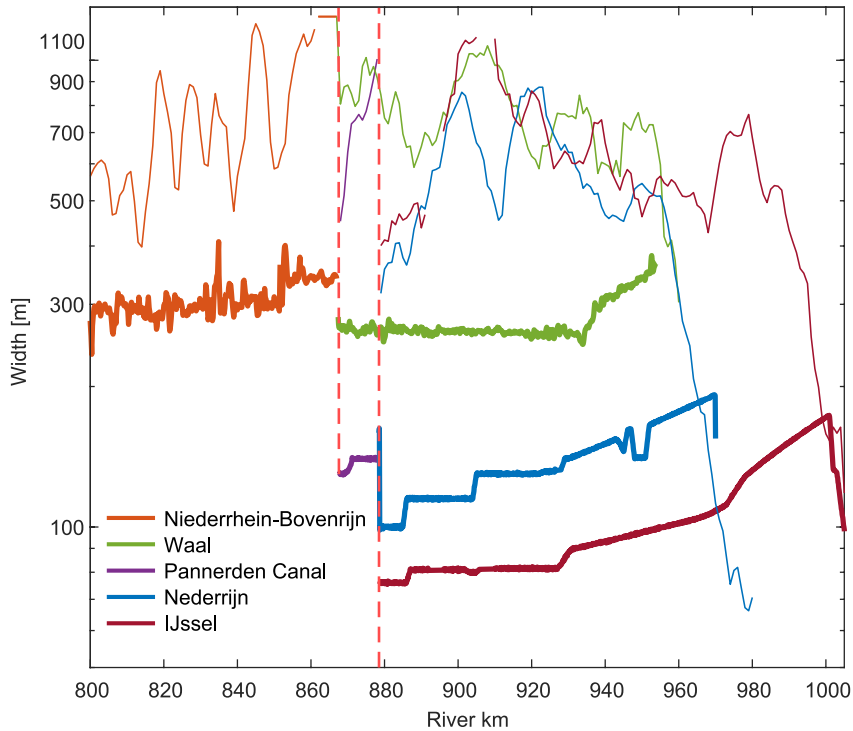


**Figure A1.** Main channel width (thick lines) and floodplain width (thin lines) of the Lower Rhine branches. Floodplain width is averaged over a moving window of 10 km.

Bed level (Figure 6) and bed surface grain size data are averaged over 5 and 10 km, respectively, unless indicated differently. Associated moving average windows do not extend across bifurcations to allow us to differentiate between the characteristics of the upstream and downstream reaches.

Water level data used in Figure 4 originate from gauging stations in Germany and the Netherlands. We adjusted the reference level to NAP (where NAP denotes Normal Amsterdam Level) for all stations and averaged the data over 24 hr to filter the effect of tides for the downstream stations. Flow depth gradient ($S_d$) in Equation 1 is computed based on water level measured at stations Pannerdense Kop, Looveer Huissen, and IJsselkop, and 2018 bed level along the Pannerden Canal.

Water discharge data were collected by Rijkswaterstaat. For discharge measurements, Ott current meters were used until 1999. ADCP has been adopted since 2000. The Ott current meter measurements have a larger inaccuracy (smaller than 20%) than ADCP measurements (smaller than 10%). The ADCP transects were traversed repeatedly at least 10 times, within at least 5% agreement to the mean discharge value. Water discharge was measured at cross-sections roughly 3–4 km upstream of the Pannerden bifurcation for Bovenrijn, approximately 1 km downstream of the Pannerden bifurcation for the Waal and Pannerden Canal, and roughly 1 km downstream of IJsselkop for Nederrijn and IJssel. We exclude water discharge data from measured water level at gauging stations, as the associated uncertainty is large (Gensen et al., 2020) and the Waal gauging station is not representative of the Waal branch due to its slightly upstream position.

The water discharge measurements do not strictly satisfy the water balance (i.e., water discharge upstream does not equal the sum of bifurcate discharges). This is because the measurements were not performed simultaneously in all branches, and floodplain discharge is typically estimated using a ratio interpolation, as vessels cannot access the shallow floodplain (Mueller et al., 2013). We compute the discharge ratio for individual measurements in the bifurcates and remove outliers that deviate by more than 10% from the mean ratio in that discharge regime. In Figure 5, each year in the *x*-axis represents a hydrologic year (e.g., year 1990 represents the time from 1 October 1989, to 30 September 1990).

The annual mean water discharge ratio in each discharge regime in Figure 5 was fitted using a piecewise linear regression with the quick succession of the 1993–1995–1998 peak flows as a breakpoint. The existence of

the breakpoint was confirmed using a moving average fit and the Loess method (see Text S1 in Supporting Information S1).

Data on channel width for the Dutch branches were provided by Rijkswaterstaat. For the German Rhine, these data were extracted from the IKSR Rhine Atlas (IKSR Rhine Atlas 2020, 2020). We have averaged the floodplain width over a 10 km window, and no averaging was applied to the main channel width. The main channel width indicates the distance between the groyne tips (Figure A1).

## Data Availability Statement

Bed level and bed surface grain size data for the Bovenrijn and Waal (1926–2018) are from Ylla Arbós (2021). Bed level data from the German Rhine are from Quick et al. (2020). The water level data from the German Rhine and Dutch Rhine are available through German Federal Waterways and Shipping Administration (WSV) and Rijkswaterstaat Central Information Service (CIV), respectively. Bed level and bed surface grain size along the Pannerden Canal, Nederrijn, and IJssel branches, and the water discharge data for the Waal and IJssel branches are available at https://doi.org/10.4121/19650873, hosted at the 4TU.ResearchData repository (Chowdhury et al., 2022).

**Acknowledgments**
This study is part of the Rivers2Morrow research program, which is funded by the Dutch Ministry of Infrastructure and Water Management (https://kbase.ncr-web.org/rivers2morrow). The authors thank the technical staff of Rijkswaterstaat for sharing the data used in this study. We thank the Editor Ellen Wohl, the Associate Editor, an anonymous reviewer and Maarten G. Kleinhans for their suggestions on the manuscript.

## References

Alexander, J. S., Wilson, R. C., & Green, W. R. (2012). *A brief history and summary of the effects of river engineering and dams on the Mississippi River system and delta* (Vol. 1375). US Department of the Interior, US Geological Survey. Retrieved from pubs.usgs.gov/circ/1375/C1375.pdf

An, C., Cui, Y., Fu, X., & Parker, G. (2017). Gravel-bed river evolution in earthquake-prone regions subject to cycled hydrographs and repeated sediment pulses. *Earth Surface Processes and Landforms*, *42*(14), 2426–2438. https://doi.org/10.1002/esp.4195

An, C., Fu, X., Wang, G., & Parker, G. (2017). Effect of grain sorting on gravel bed river evolution subject to cycled hydrographs: Bed load sheets and breakdown of the hydrograph boundary layer. *Journal of Geophysical Research: Earth Surface*, *122*(8), 1513–1533. https://doi.org/10.1002/2016jf003994

Arkesteijn, L., Blom, A., Czapiga, M. J., Chavarrías, V., & Labeur, R. J. (2019). The quasi-equilibrium longitudinal profile in backwater reaches of the engineered alluvial river: A space-marching method. *Journal of Geophysical Research: Earth Surface*, *124*(11), 2542–2560. https://doi.org/10.1029/2019jf005195

Arkesteijn, L., Blom, A., & Labeur, R. J. (2021). A rapid method for modeling transient river response under stochastic controls with applications to sea level rise and sediment nourishment. *Journal of Geophysical Research: Earth Surface*, *126*(12). https://doi.org/10.1029/2021jf006177

Asmerom, K. J. H. K. (2001). *Bodemsprongen Pannerdensche Kop en IJsselkop: De 1-dimensionale lokale bodemligging bij splitsingspunten van rivieren* (Master's thesis). Delft University of Technology. Retrieved from https://repository.tudelft.nl/islandora/object/uuid:07fb5d94-8370-4103-81a4-279c9db307c9

Bertoldi, W. (2012). Life of a bifurcation in a gravel-bed braided river. *Earth Surface Processes and Landforms*, *37*(12), 1327–1336. https://doi.org/10.1002/esp.3279

Blom, A. (2008). Different approaches to handling vertical and streamwise sorting in modeling river morphodynamics. *Water Resources Research*, *44*(3), W03415. https://doi.org/10.1029/2006wr005474

Blom, A., Arkesteijn, L., Chavarrías, V., & Viparelli, E. (2017). The equilibrium alluvial river under variable flow and its channel-forming discharge. *Journal of Geophysical Research: Earth Surface*, *122*(10), 1924–1948. https://doi.org/10.1002/2017jf004213

Blom, A., Chavarrías, V., Ferguson, R. I., & Viparelli, E. (2017). Advance, retreat, and halt of abrupt gravel-sand transitions in alluvial rivers. *Geophysical Research Letters*, *44*(19), 9751–9760. https://doi.org/10.1002/2017gl074231

Blom, A., & Parker, G. (2004). Vertical sorting and the morphodynamics of bed form-dominated rivers: A modeling framework. *Journal of Geophysical Research*, *109*(F2), 1–15. https://doi.org/10.1029/2003jf000069

Blom, A., Ribberink, J. S., & de Vriend, H. J. (2003). Vertical sorting in bed forms: Flume experiments with a natural and a trimodal sediment mixture. *Water Resources Research*, *39*(2), 1025. https://doi.org/10.1029/2001wr001088

Blom, A., Viparelli, E., & Chavarrías, V. (2016). The graded alluvial river: Profile concavity and downstream fining. *Geophysical Research Letters*, *43*(12), 6285–6293. https://doi.org/10.1002/2016gl068898

Bolla Pittaluga, M., Repetto, R., & Tubino, M. (2003). Channel bifurcation in braided rivers: Equilibrium configurations and stability. *Water Resources Research*, *39*(3), 1046. https://doi.org/10.1029/2001wr001112

Cenderelli, D. A., & Wohl, E. E. (2003). Flow hydraulics and geomorphic effects of glacial-lake outburst floods in the Mount Everest region, Nepal. *Earth Surface Processes and Landforms*, *28*(4), 385–407. https://doi.org/10.1002/esp.448

Chatanantavet, P., & Lamb, M. P. (2014). Sediment transport and topographic evolution of a coupled river and river plume system: An experimental and numerical study. *Journal of Geophysical Research: Earth Surface*, *119*(6), 1263–1282. https://doi.org/10.1002/2013jf002810

Chatanantavet, P., Lamb, M. P., & Nittrouer, J. A. (2012). Backwater controls of avulsion location on deltas. *Geophysical Research Letters*, *39*(1), L01402. https://doi.org/10.1029/2011GL050197

Chowdhury, M. K., Blom, A., Ylla Arbós, C., Verbeek, M. C., Schropp, M. H. I., & Schielen, R. M. J. (2022). *Bed elevation, bed surface grain size (D50 and D90), and water discharge- Waal, Pannerden Channel, Nederrijn, and IJssel, 1928–2020*. 4TU.ResearchData. https://doi.org/10.4121/19650873

Cleveland, W. S. (1979). Robust locally weighted regression and smoothing scatterplots. *Journal of the American Statistical Association*, *74*(368), 829–836. https://doi.org/10.1080/01621459.1979.10481038

De Vriend, H. (2015). The long-term response of rivers to engineering works and climate change. *Proceedings of the Institution of Civil Engineers*, *168*(3), 139–144. https://doi.org/10.1680/cien.14.00068

Dutta, S., Wang, D., Tassi, P., & Garcia, M. H. (2017). Three-dimensional numerical modeling of the Bulle effect: The nonlinear distribution of near-bed sediment at fluvial diversions. *Earth Surface Processes and Landforms*, *42*(14), 2322–2337. https://doi.org/10.1002/esp.4186

East, A. E., Logan, J. B., Mastin, M. C., Ritchie, A. C., Bountry, J. A., Magirl, C. S., & Sankey, J. B. (2018). Geomorphic evolution of a gravel-bed river under sediment-starved versus sediment-rich conditions: River response to the world's largest dam removal. *Journal of Geophysical Research: Earth Surface*, *123*(12), 3338–3369. https://doi.org/10.1029/2018jf004703

Edmonds, D. A. (2012). Stability of backwater-influenced river bifurcations: A study of the Mississippi-Atchafalaya system. *Geophysical Research Letters*, *39*(8), L08402. https://doi.org/10.1029/2012gl051125

Engelund, F., & Hansen, E. (1967). *A monograph on sediment transport in alluvial streams* (Vol. 10). Technical University of Denmark Østervoldgade. Retrieved from http://resolver.tudelft.nl/uuid:81101b08-04b5-4082-9121-861949c336c9

Exner, F. M. (1920). Zur Physik der Dünen. *Akademie der Wissenschaften in Wien. Mathematisch-Naturwissenschaftliche Klasse*, *129*(2a), 929–952.

Ferrand, J. H. (1847). *Memorie over de verdeeling der wateren van den Boven-Rijn, tusschen de Waal, den Neder-Rijn en den IJssel*. Ter Algemeene Lands Drukkerij. Retrieved from http://books.google.com/books?vid=KBNL:UBA000036956

Frings, R. M. (2011). Sedimentary characteristics of the gravel-sand transition in the River Rhine. *Journal of Sedimentary Research*, *81*(1), 52–63. https://doi.org/10.2110/jsr.2011.2

Frings, R. M., Banhold, K., & Evers, I. (2015). *Sedimentbilanz des Oberen Rheindeltas für den Zeitraum 1991–2010* (in German) (Technical Report No. 2015.019). Institut für Wasserbau und Wasserwirtschaft, RWTH Aachen.

Frings, R. M., Berbee, B. M., Erkens, G., Kleinhans, M. G., & Gouw, M. J. P. (2009). Human-induced changes in bed shear stress and bed grain size in the River Waal (The Netherlands) during the past 900 years. *Earth Surface Processes and Landforms*, *34*(4), 503–514. https://doi.org/10.1002/esp.1746

Frings, R. M., Döring, R., Beckhausen, C., Schüttrumpf, H., & Vollmer, S. (2014). Fluvial sediment budget of a modern, restrained river: The lower reach of the Rhine in Germany. *Catena*, *122*, 91–102. https://doi.org/10.1016/j.catena.2014.06.007

Frings, R. M., Hillebrand, G., Gehres, N., Banhold, K., Schriever, S., & Hoffmann, T. (2019). From source to mouth: Basin-scale morphodynamics of the Rhine River. *Earth-Science Reviews*, *196*, 102830. https://doi.org/10.1016/j.earscirev.2019.04.002

Frings, R. M., & Kleinhans, M. G. (2008). Complex variations in sediment transport at three large river bifurcations during discharge waves in the River Rhine. *Sedimentology*, *55*(5), 1145–1171. https://doi.org/10.1111/j.1365-3091.2007.00940.x

Gensen, M. R. A., Warmink, J. J., Huthoff, F., & Hulscher, S. J. M. H. (2020). Feedback mechanism in bifurcating river systems: The effect on water-level sensitivity. *Water*, *12*(7), 1915. https://doi.org/10.3390/w12071915

Gervasi, A. A., Pasternack, G. B., & East, A. E. (2021). Flooding duration and volume more important than peak discharge in explaining 18 years of gravel–cobble river change. *Earth Surface Processes and Landforms*, *46*(15), 3194–3212. https://doi.org/10.1002/esp.5230

Gilbert, G. K. (1877). *Geology of the Henry Mountains*. US Geological Survey. https://doi.org/10.3133/70038096

Gruijters, S. H. L. L., Gunnink, J., Hettelaar, J. J. M., De Kleine, M. P. E., Maljers, D., & Veldkamp, J. G. (2003). *Kartering ondergrond IJsselkop, fase 3, eindrapport* (in Dutch) (Technical Report No. NITG 03-120-B). Nederlands Instituut voor Toegepaste Geowetenschappen TNO. Retrieved from https://open.rws.nl/open-overheid/onderzoeksrapporten/@141923/kartering-ondergrond-ijsselkop-fase-3/

Gruijters, S. H. L. L., Veldkamp, J. G., Gunnink, J., & Bosch, J. H. A. (2001). *De lithologische en sedimentologische opbouw van de ondergrond van de Pannerdensche Kop* (in Dutch) (Technical Report No. NITG 01-166-B). Nederlands Instituut voor Toegepaste Geowetenschappen TNO. Retrieved from https://open.rws.nl/open-overheid/onderzoeksrapporten/@195118/lithologische-sedimentologische-opbouw/

Gupta, N., Kleinhans, M. G., Addink, E. A., Atkinson, P. M., & Carling, P. A. (2014). One-dimensional modeling of a recent Ganga avulsion: Assessing the potential effect of tectonic subsidence on a large river. *Geomorphology*, *213*, 24–37. https://doi.org/10.1016/j.geomorph.2013.12.038

Habersack, H., Hein, T., Stanica, A., Liska, I., Mair, R., Jäger, E., et al. (2016). Challenges of river basin management: Current status of, and prospects for, the River Danube from a river engineering perspective. *Science of the Total Environment*, *543*, 828–845. https://doi.org/10.1016/j.scitotenv.2015.10.123

Hauer, C., & Habersack, H. (2009). Morphodynamics of a 1000-year flood in the Kamp River, Austria, and impacts on floodplain morphology. *Earth Surface Processes and Landforms*, *34*(5), 654–682. https://doi.org/10.1002/esp.1763

Havinga, H. (2020). Towards sustainable river management of the Dutch Rhine River. *Water*, *12*(6), 1827. https://doi.org/10.3390/w12061827

Hesselink, A. W. (2002). *History makes a river: Morphological changes and human interference in the River Rhine, The Netherlands* (Vol. 292). Nederlandse Geografische Studies. Retrieved from tudelft.on.worldcat.org/oclc/1017492654

Hesselink, A. W., Kleinhans, M. G., & Boreel, G. L. (2006). Historic discharge measurements in three Rhine branches. *Journal of Hydraulic Engineering*, *132*(2), 140–145. https://doi.org/10.1061/(asce)0733-9429(2006)132:2(140)

Huckleberry, G. (1994). Contrasting channel response to floods on the middle Gila River, Arizona. *Geology*, *22*(12), 1083–1086. https://doi.org/10.1130/0091-7613(1994)022<1083:ccrtfo>2.3.co;2

IKSR Rhine Atlas 2020. (2020). IKSR – Internationale Kommission zum Schutz des Rheins. Retrieved from geoportal.bafg.de/arcportal/apps/webappviewer/index.html?id=b6085b53b6d84cd39cff4bf5eb7f3f40

Jansen, P., Van Bendegom, L., Van den Berg, J. H., De Vries, M. B., & Zanen, A. (1979). *Principles of river engineering: The non-tidal alluvial river*. Pitman London.

Kleinhans, M. G. (2001). The key role of fluvial dunes in transport and deposition of sand–gravel mixtures, a preliminary note. *Sedimentary Geology*, *143*(1–2), 7–13. https://doi.org/10.1016/s0037-0738(01)00109-9

Kleinhans, M. G. (2005). Dune-phase fluvial transport and deposition model of gravelly sand. In *Fluvial sedimentology VII* (pp. 75–97). Blackwell Publishing Ltd. https://doi.org/10.1002/9781444304350.ch5

Kleinhans, M. G., Cohen, K. M., Hoekstra, J., & IJmker, J. M. (2011). Evolution of a bifurcation in a meandering river with adjustable channel widths, Rhine delta apex, The Netherlands. *Earth Surface Processes and Landforms*, *36*(15), 2011–2027. https://doi.org/10.1002/esp.2222

Kleinhans, M. G., Ferguson, R. I., Lane, S. N., & Hardy, R. J. (2013). Splitting rivers at their seams: Bifurcations and avulsion. *Earth Surface Processes and Landforms*, *38*(1), 47–61. https://doi.org/10.1002/esp.3268

Kleinhans, M. G., Jagers, H. R. A., Mosselman, E., & Sloff, C. J. (2008). Bifurcation dynamics and avulsion duration in meandering rivers by one-dimensional and three-dimensional models. *Water Resources Research*, *44*(8), W08454. https://doi.org/10.1029/2007wr005912

Kleinhans, M. G., Wilbers, A. W. E., & Ten Brinke, W. B. M. (2007). Opposite hysteresis of sand and gravel transport upstream and downstream of a bifurcation during a flood in the River Rhine, The Netherlands. *Netherlands Journal of Geosciences*, *86*(3), 273–285. https://doi.org/10.1017/s0016774600077854

Klein Tank, A., Beersma, J., Bessembinder, J., Van den Hurk, B., & Lenderink, G. (2014). *KNMI'14: Climate scenarios for The Netherlands: A guide for professionals inclimate adaption*. KNMI, De Bilt. Retrieved from https://edepot.wur.nl/328690

Lane, E. W. (1955). The importance of fluvial morphology in hydraulic engineering. *Proceedings of the American Society of Civil Engineers*, *81*(754), 1–17.

Lisenby, P. E., Croke, J., & Fryirs, K. A. (2017). Geomorphic effectiveness: A linear concept in a non-linear world. *Earth Surface Processes and Landforms*, *43*(1), 4–20. https://doi.org/10.1002/esp.4096

Mackin, J. H. (1948). Concept of the graded river. *Geological Society of America Bulletin*, *59*(5), 463. https://doi.org/10.1130/0016-7606(1948)59[463:cotgr]2.0.co;2

Magilligan, F. J. (1992). Thresholds and the spatial variability of flood power during extreme floods. *Geomorphology*, *5*(3–5), 373–390. https://doi.org/10.1016/0169-555x(92)90014-f

Mao, L. (2018). The effects of flood history on sediment transport in gravel-bed rivers. *Geomorphology*, *322*, 196–205. https://doi.org/10.1016/j.geomorph.2018.08.046

McKee, E. D., Crosby, E. J., & Berryhill, H. L. (1967). Flood deposits, Bijou Creek, Colorado, June 1965. *Journal of Sedimentary Research*, *37*(3), 829–851. https://doi.org/10.1306/74d717b2-2b21-11d7-8648000102c1865d

Mendoza, A., Berezowsky, M., Caballero, C., & Arganis-Juárez, M. (2021). Alteration of the flow distribution at a river bifurcation caused by a system of upstream dams: Case of the Grijalva River basin, Mexico. *Earth Surface Processes and Landforms*, *47*(2), 509–521. https://doi.org/10.1002/esp.5265

Mendoza, A., Soto-Cortes, G., Priego-Hernandez, G., & Rivera-Trejo, F. (2019). Historical description of the morphology and hydraulic behavior of a bifurcation in the lowlands of the Grijalva River Basin, Mexico. *Catena*, *176*, 343–351. https://doi.org/10.1016/j.catena.2019.01.033

Mueller, D. S., Wagner, C. R., Rehmel, M. S., Oberg, K. A., & Rainville, F. (2013). *Measuring discharge with acoustic Doppler current profilers from a moving boat*. US Geological Survey. https://doi.org/10.3133/tm3a22

Parker, G., & Andrews, E. D. (1985). Sorting of bed load sediment by flow in meander bends. *Water Resources Research*, *21*(9), 1361–1373. https://doi.org/10.1029/wr021i009p01361

Parker, G., & Klingeman, P. C. (1982). On why gravel bed streams are paved. *Water Resources Research*, *18*(5), 1409–1423. https://doi.org/10.1029/wr018i005p01409

Parker, G., Shimizu, Y., Wilkerson, G. V., Eke, E. C., Abad, J. D., Lauer, J. W., et al. (2010). A new framework for modeling the migration of meandering rivers. *Earth Surface Processes and Landforms*, *36*(1), 70–86. https://doi.org/10.1002/esp.2113

Parker, G., & Sutherland, A. J. (1990). Fluvial armor. *Journal of Hydraulic Research*, *28*(5), 529–544. https://doi.org/10.1080/00221689009499044

Parker, G., & Toro-Escobar, C. M. (2002). Equal mobility of gravel in streams: The remains of the day. *Water Resources Research*, *38*(11), 46-1–46-8. https://doi.org/10.1029/2001wr000669

Petit, F., Poinsart, D., & Bravard, J. P. (1996). Channel incision, gravel mining and bedload transport in the Rhône River upstream of Lyon, France ("Canal de Miribel"). *Catena*, *26*(3–4), 209–226. https://doi.org/10.1016/0341-8162(95)00047-x

Pinter, N., van der Ploeg, R. R., Schweigert, P., & Hoefer, G. (2006). Flood magnification on the River Rhine. *Hydrological Processes*, *20*(1), 147–164. https://doi.org/10.1002/hyp.5908

Pizzuto, J. E. (1994). Channel adjustments to changing discharges, Powder River, Montana. *Geological Society of America Bulletin*, *106*(11), 1494–1501. https://doi.org/10.1130/0016-7606(1994)106⟨1494:catcdp⟩2.3.co;2

Quick, I., König, F., Baulig, Y., Schriever, S., & Vollmer, S. (2020). Evaluation of depth erosion as a major issue along regulated rivers using the classification tool Valmorph for the case study of the Lower Rhine. *International Journal of River Basin Management*, *18*(2), 191–206. https://doi.org/10.1080/15715124.2019.1672699

Saint Venant, A. J. C. B. (1871). Théorie du mouvement non permanent des eaux, avec application aux crues des rivières et à l'introduction de marées dans leur lit. *Comptes Rendus de l'Académie des Sciences de Paris*, *73*(99), 237–240. (in French).

Schielen, R. M. J., & Blom, A. (2018). A reduced complexity model of a gravel-sand river bifurcation: Equilibrium states and their stability. *Advances in Water Resources*, *121*, 9–21. https://doi.org/10.1016/j.advwatres.2018.07.010

Schielen, R. M. J., Jesse, P., & Bolwidt, L. J. (2007). On the use of flexible spillways to control the discharge ratio of the Rhine in The Netherlands: Hydraulic and morphological observations. *Netherlands Journal of Geosciences - Geologie en Mijnbouw*, *86*(1), 77–88. https://doi.org/10.1017/s0016774600021338

Sholtes, J. S., Yochum, S. E., Scott, J. A., & Bledsoe, B. P. (2018). Longitudinal variability of geomorphic response to floods. *Earth Surface Processes and Landforms*, *43*(15), 3099–3113. https://doi.org/10.1002/esp.4472

Sloff, K., & Mosselman, E. (2012). Bifurcation modelling in a meandering gravel-sand bed river. *Earth Surface Processes and Landforms*, *37*(14), 1556–1566. https://doi.org/10.1002/esp.3305

Sperna Weiland, F., Hegnauer, M., Bouaziz, L., & Beersma, J. (2015). *Implications of the KNMI'14 climate scenarios for the discharge of the Rhine and Meuse*. Deltares. Retrieved from https://publications.deltares.nl/1220042_000.pdf

Stumpe, J. (2009). *Nationaal Waterplan 2009–2015 (No. 395934)*. Rijkswaterstaat. Retrieved from https://www.helpdeskwater.nl/onderwerpen/wetgeving-beleid/nationaal/nationaal-waterplan/

Syvitski, J. P. M., & Brakenridge, G. R. (2013). Causation and avoidance of catastrophic flooding along the Indus River, Pakistan. *Geological Society of America Today*, *23*(1), 4–10. https://doi.org/10.1130/GSATG165A.1

Te Linde, A. H., Aerts, J. C. J. H., Bakker, A. M. R., & Kwadijk, J. C. J. (2010). Simulating low-probability peak discharges for the Rhine basin using resampled climate modeling data. *Water Resources Research*, *46*(3), W03512. https://doi.org/10.1029/2009wr007707

Ten Brinke, W. B. M. (1997). *De bodemsamenstelling van Waal en IJssel in de jaren 1966, 1976, 1984 en 1995. RIZA rapport, 97.009*. Netherlands Institute for Inland Water Management and Waste Water Treatment. Retrieved from https://open.rws.nl/open-overheid/onderzoeksrapporten/@69122/bodemsamenstelling-waal-ijssel-jaren/

Ten Brinke, W. B. M. (2005). *The Dutch Rhine: A restrained river*. Veen Magazines. Retrieved from books.google.nl/books?id=E_tcAgAACAAJ

Ten Brinke, W. B. M., Schoor, M. M., Sorber, A. M., & Berendsen, H. J. A. (1998). Overbank sand deposition in relation to transport volumes during large-magnitude floods in the Dutch sand-bed Rhine river system. *Earth Surface Processes and Landforms*, *23*(9), 809–824. https://doi.org/10.1002/(sici)1096-9837(199809)23:9⟨809::aid-esp890⟩3.0.co;2-1

Van de Lageweg, W. I., van Dijk, W. M., Baar, A. W., Rutten, J., & Kleinhans, M. G. (2014). Bank pull or bar push: What drives scroll-bar formation in meandering rivers? *Geology*, *42*(4), 319–322. https://doi.org/10.1130/g35192.1

Van de Ven, G. P. (1976). *Aan de wieg van Rijkswaterstaat: Wordingsgeschiedenis van het Pannerdens Kanaal*. Walburg Pers. Retrieved from https://open.rws.nl/open-overheid/onderzoeksrapporten/@139132/wieg-rijkswaterstaat/

Van Doornik, W., den Daas, J., Pfaff-Wagenaar, M., Dorenbosch, M., Liefveld, W., & Grutters, B. (2019). *Stuwbeheer Nederrijn – Lek: Optimalisatiestudie vanuit de KRW-functie* (in Dutch). Rijkswaterstaat. Retrieved from https://open.rws.nl/open-overheid/onderzoeksrapporten/@154234/stuwbeheer-nederrijn-lek/

Van Stokkom, H. T. C., Smits, A. J. M., & Leuven, R. S. E. W. (2005). Flood defense in The Netherlands. *Water International*, *30*(1), 76–87. https://doi.org/10.1080/02508060508691839

Visser, P. J. (2000). *Bodemontwikkeling Rijnsysteem: Een verkenning van omvang, oorzaken, toekomstige ontwikkelingen en mogelijke maatregelen*. TU Delft, Department Hydraulic Engineering. Retrieved from https://open.rws.nl/open-overheid/onderzoeksrapporten/@195133/bodemontwikkeling-rijnsysteem-verkenning/

Wang, Z. B., De Vries, M., Fokkink, R. J., & Langerak, A. (1995). Stability of river bifurcations in 1D morphodynamic models. *Journal of Hydraulic Research*, *33*(6), 739–750. https://doi.org/10.1080/00221689509498549

Wolfert, H. P. (2001). *Geomorphological change and river rehabilitation: Case studies on lowland fluvial systems in The Netherlands* (Doctoral dissertation). Alterra Green World Research. Retrieved from dspace.library.uu.nl/bitstream/handle/1874/540/full.pdf

Ylla Arbós, C. (2021). *Bed elevation and bed surface grain size (d50) Bovenrijn and Waal, 1926–2020*. 4TU.ResearchData. https://doi.org/10.4121/13065359.V2

Ylla Arbós, C., Blom, A., Sloff, C. J., & Schielen, R. M. J. (2023). Centennial channel response to climate change in an engineered river. *Geophysical Research Letters*, e2023GL103000. https://doi.org/10.1029/2023GL103000

Ylla Arbós, C., Blom, A., Viparelli, E., Reneerkens, M., Frings, R. M., & Schielen, R. M. J. (2021). River response to anthropogenic modification: Channel steepening and gravel front fading in an incising river. *Geophysical Research Letters*, *48*(4), e2020GL091338. https://doi.org/10.1029/2020gl091338

Yochum, S. E., Sholtes, J. S., Scott, J. A., & Bledsoe, B. P. (2017). Stream power framework for predicting geomorphic change: The 2013 Colorado Front Range flood. *Geomorphology*, *292*, 178–192. https://doi.org/10.1016/j.geomorph.2017.03.004

Yossef, M., Becker, A., & Deák, G. (2016). Modelling large scale and long term morphological response to engineering interventions at river bifurcation. In *River flow 2016*. CRC Press. https://doi.org/10.1201/9781315644479-214

Yousefi, S., Mirzaee, S., Keesstra, S., Surian, N., Pourghasemi, H. R., Zakizadeh, H. R., & Tabibian, S. (2018). Effects of an extreme flood on river morphology (case study: Karoon River, Iran). *Geomorphology*, *304*, 30–39. https://doi.org/10.1016/j.geomorph.2017.12.034

## References From the Supporting Information

NIST/SEMATECH e-Handbook of Statistical Methods. (2020). Loess (aka lowess). https://doi.org/10.18434/M32189

Ylla Arbós, C., Blom, A., Van Vuren, S., & Schielen, R. M. J. (2019). *Bed level change in the upper rhine delta since 1926 and rough extrapolation to 2050*. Delft University of Technology. Retrieved from https://kbase.ncr-web.org/rivers2morrow/outputs/bed-level-change-in-the-upper-rhine-delta-since-1926-and-rough-extrapolation-to-2050/